Results and Discussion

Chapter (III)
The Spectral and Voltammetric Characterization of The Organic Ligands

3.1. The electronic absorption spectra of azo dye and Schiff base compounds in different organic solvents

The electronic absorption spectra of azo dye and Schiff base compounds derived from 6-amino-2,3-dihydroxyquinoxaline were studied in six organic solvents, the solvents included ethanol, acetonitrile, DMF, 1,4-dioxane, n-hexane and acetone. The changes in extinction and displacements of absorption bands can take place according to the nature of solvent used. This displacement includes either red or blue shifts on going from nonpolar to polar solvent. These effects are due to the following reasons:

1- The physical properties of the organic solvent such as dipole moment, dielectric constant, refractive index and its ability to interact through hydrogen bonding with the solute molecules.

2- The difference in solvation energy from one solvent to another and also on going from the ground to the excited state during excitation in the same solvent.

3- The changes in polarities and dipole moments of the solute on excitation.

The studies reveal that the electronic absorption spectra involve bands due to electronic transitions within the various moieties **locally excited (LE)** attached either to the azo group or to the azomethine group leading to absorption in the UV region and band corresponding to the electronic excitation of the π and n-electrons on the (-N=N-) and (-CH=N-) systems which can be activated by **charge transfer (CT)** interactions. The spectra of the ligands under investigation can be classified into two regions. The first one below $\simeq$ 310 nm being attributed to the localized transitions of substituted aromatic rings. The second region is located above $\simeq$ 310 nm and can be assigned to transitions within the (-N=N-) or (-CH=N-) systems, which are influenced by the different types of interamolecular charge transfer liable to occur within the molecules.

3.1.1. The electronic absorption spectra of azo dyes in ethanol

The electronic absorption spectra of azo dye ligands (I_{a-c}) in ethanol are shown in Fig. (2). The electronic spectra of the azo compounds under investigation show mainly three absorption bands within absorption region 190-500 nm. The first band at 263 and 269 nm for ligands I_a and I_b which has ε_{max} 0.90 x 10^4 and 0.24 x 10^4 L mol^{-1} cm^{-1} respectively. This band is due to moderate energy transition ($^1B_a \leftarrow {}^1A$) state in the naphthyl moieties for ligands I_a and I_b. The second band has λ_{max} at wavelength 284, 273 and 242 nm and ε_{max} 0.81 x 10^4, 0.24 x 10^4 and 0.82 x 10^4 L mol^{-1} cm^{-1} for I_a, I_b and I_c, respectively. These bands are attributed to the transition within the quinoxaline moiety and the π-π* transition ($^1L_b \leftarrow {}^1A$) for aromatic systems. Also, the first band has high extinction value and is solvent insensitive. The third band at 340, 330 and 317 nm with ε_{max} 0.64 x 10^4, 0.12 x 10^4 and 0.10 x 10^4 L mol^{-1} cm^{-1} for ligands I_a, I_b and I_c respectively is very sensitive to solvent polarity. This band is probably of the charge transfer type. For all ligands I_{a-c} we observed a shoulder at 423, 390 and 364 nm for I_a, I_b and I_c which can be explained the bases of an azo-hydrazo tautomeric equilibrium(3) of this compounds which can be represented as follows:

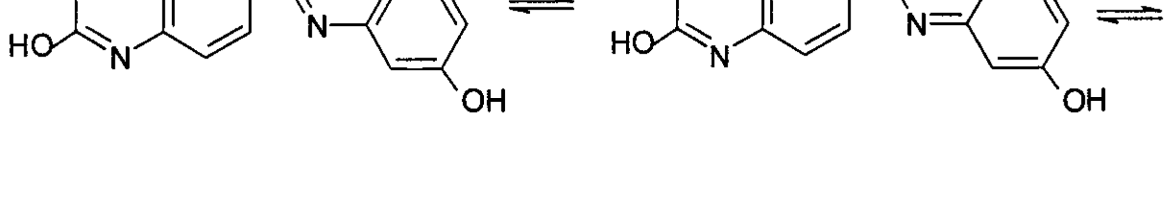

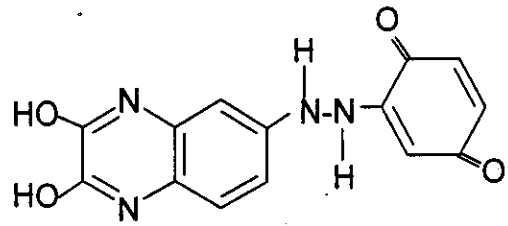

From Fig. (2) the CT band of compound I_c splits to two bands one of them at 293 nm and the other at 317 nm and this can be attributed to the intramolecular hydrogen bonds formed in this ligands which can be represented as follows:

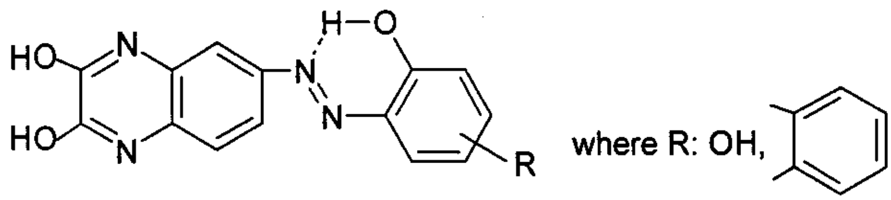

The spectral data of these ligands are given in Table (2).

3.1.2. The electronic absorption spectra of Schiff bases in ethanol

The electronic absorption spectra of Schiff bases $II_{a\text{-}c}$ under investigation in ethanol display bands as shown in Fig. (2).

The first band is observed at 230 and 225 (sh) nm with ε_{max} 0.2 x 10^4 and 0.52 x 10^4 L mol^{-1} cm^{-1} for II_a and II_b respectively, and this band due to transition ($^1L_a \leftarrow {}^1A$) state in the phenyl ring for II_a and transition ($^1B_a \leftarrow {}^1A$) state in naphthyl system for II_b. The second band observed at 277, 275 and 250 nm with ε_{max} 0.23 x 10^4, 0.36 x 10^4 and 0.71 x 10^4 L mol^{-1} cm^{-1} for II_a, II_b and II_c, respectively, may be due to π-π^* transition of type ($^1L_b \leftarrow {}^1A$) state occuring in the quinoxaline system. We found that this band is slightly influenced by organic solvents. The third band at 330, 330 and 311 nm with ε_{max} 0.18 x 10^4, 0.30 x 10^4 and 1.30 x 10^4 L mol^{-1} cm^{-1} for II_a, II_b and II_c, respectively, is due to the n-π^* transition which occurs in the azomethine system. We observe from Fig. (2) that there is a shoulder at 397, 415 and 425 nm for ligands II_a, II_b and II_c respectively which may be due to the delodization of hydrogen atom from (OH) group to give keto form which can be represented as follows:

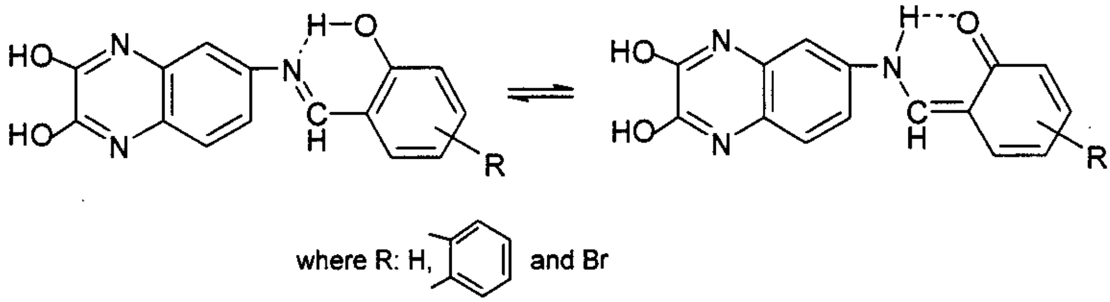

The spectral data of compounds II_{a-c} are listed in Table (3).

3.2. The electronic absorption spectra of azo compounds under investigation in different organic solvents

The electronic absorption spectra of azo dyes I_{a-c} were recorded in ethanol, acetonitril, dimethyl formamide (DMF), n-hexane, acetone and 1,4-dioxane as shown in Figs. (3-5). For the spectra of azo dyes ligands, its apparent that, the spectrum of each compound exhibits mainly two regions. The first region observed in the range 190-300 nm can be attributed to the localized transitions within phenyl and quinoxaline moieties. The second region appearing in range above 300 nm ascribed to CT transition within the molecule through azo group linkage. The first band which observed at 272 and 234 nm with ε_{max} 0.40 x 10^4 and 1.14 x 10^4 L mol^{-1} cm^{-1} respectively for I_b and I_c is due to the π-π^* transition which occurs within the quinoxaline system, other bands in the different organic solvents for the azo dye ligands are listed in Table (2). From the spectra of azo dye ligands (I_{a-c}) it is apparent that, the spectrum of each compound exhibits mainly three bands. We observed that both intramolecular CT band and LE band are solvent sensitive but by different ways. For ligands I_a and I_b the polar solvent exhibits a band with slight red shift which is referred to the π-π* transition occuring in azo groups (N=N). But for ligand I_c there are no changes observed in the position of CT band for both polar on non polar solvents as shown in Fig. (5).

3.3. The electronic absorption spectra of Schiff base compounds under investigation in different organic solvents

It is apparent that the position and extinctions of bands appearing in the UV and visible regions are dependent on the polarity of the medium and the nature of substituents on the ligand molecules. The general trend observed shows that all π-π* transitions within the molecules are influenced by the n-electrons on the –N=CH- group and an intramolecular change transfer. The visible band is slightly red shifted in ethanol than in n-hexane. This small red shift can be explained on the basis that the ethanol molecules may associate with (-OH) group through H-bond formation and this observed from the positions of absorption bands of Schiff base compounds after dissolving in different organic solvent as shown in Figs. (6-8).

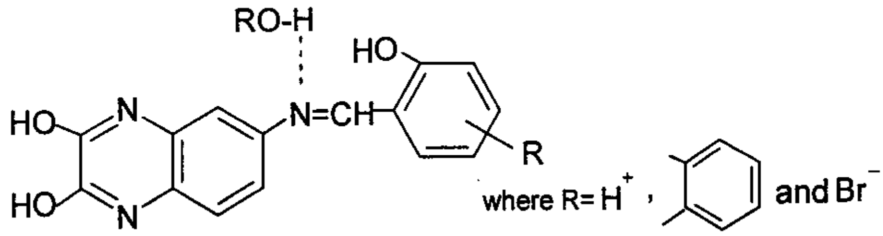

For the spectra of Schiff base compounds, it is apparent that the spectrum of each compound exhibits mainly three bands as shown in Table (3), for DMF as organic solvent, the first band at 335 (sh) and 342 nm with ε_{max} 0.28 x 10^4 and 0.24 x 10^4 L mol^{-1} cm^{-1} for ligand II_a and II_b respectively, and this band due to the π-π* transition of phenyl ring, whereas the second band at 400, 413 and 311 nm with ε_{max} 0.36 x 10^4,

0.42×10^4 and 1.11×10^4 L mol^{-1} cm^{-1} is due to the electronic transition occurring within quinoxaline system. The third band which appeared at 436, 466 and 335 nm with ε_{max} 0.48×10^4, 0.44×10^4 and 0.60×10^4 L mol^{-1} cm^{-1} for ligands II_a, II_b and II_c respectively is due to the CT transition which occurred through the azomethine group in Schiff base compounds. We observe that these bands appear at higher wavelength which may be due to intermolecular hydrogen bond between ligand and DMF.

In some case, although ethanol is a solvent with relatively high polarity compared to 1,4-dioxane and n-hexane, the UV band appearing in ethanol exhibits a slight blue shift compared to nonpolar solvents. This behavior may be attributed to the blocking of the n-electrons by ethanol molecules hence blocking the resonance on the aromatic ring. This renders the excitation of the π-electrons on the phenyl group more difficult, thus requiring higher energy, hence the small blue shift of such bands in ethanol(91).

?

The shift in λ_{max} can be discussed in term of the solvent polarity viz dielectric constant and the possibility of formation of an intermolecular hydrogen bonds between ligand and solvent molecules.

The relation which governs this behavior was given by **Gati** and **Szalay**(92) in the form of:

$$\Delta\bar{\nu} = (a-b)\left(\frac{n^2-1}{2n^2+1}\right) + b\left(\frac{D-1}{D+1}\right)$$

In which a and b are constants depending on the nature of the solute, n is the refractive index and D is the dielectric constant of the medium.

According to this relation, the plot of $\Delta\bar{\nu}$ as a function of the term would be a linear relation if the dielectric force is predominant. But the relation shows no straight lines indicating that the dielectric constant of the medium is not the main factor governing band shift. So, the main factors are the polarization forces and the solvent-solute interactions leading to intermolecular hydrogen bonding especially with protic solvents as well as changes in the solvation energy of both ground and excited states[93].

For the spectra of Schiff base ligands (II_{a-c}) its apparent that, the spectrum of each component exhibits mainly two bands except in case of ligand II_c where only one band is observed in UV region with a shoulder at longer wavelength. We observe that both intramolecular CT band and LE band are solvent sensitive but in different ways. For ligands II_a and II_b the polar solvents have CT band with slight red shift compared with the nonpolar solvent and this CT band is referred to the π-π^* transition which occurs within the azometheme group.

Table (2): ***The spectral data of ligands I_{a-c} in different organic solvents***

Solvent	I_a						
	A		B		C		D
	λ_{max} (nm)	ε_{max} x 10^4	λ_{max} (nm)	ε_{max} x 10^4	λ_{max} (nm)	ε_{max} x 10^4	λ_{max} (nm)
Ethanol	263	0.90	284	0.81	340	0.68	423 (sh)
Acetonitril	-	-	323	1.10	340	1.10	463 (sh)
DMF	-	-	284	0.49	344	0.28	453 (sh)
n-Hexane	210	0.32	263	0.17	343	0.08	410 (sh)
Acetone	-	-	-	-	340	0.46	435 (sh)
1,4-Dioxane	280	1.16	325	0.59	340	0.59	470 (sh)

Solvent	I_b						
	A		B		C		D
	λ_{max} (nm)	ε_{max} x 10^4	λ_{max} (nm)	ε_{max} x 10^4	λ_{max} (nm)	ε_{max} x 10^4	λ_{max} (nm)
Ethanol	269	0.24	273	0.24	330	0.12	390 (sh)
Acetonitril	-	-	272	0.40	329	0.20	392 (sh)
DMF	-	-	270	0.90	376	0.13	440 (sh)
n-Hexane	-	-	271	0.02	326	0.09	405 (sh)
Acetone	-	-	332	0.18	371	0.09	392 (sh)
1,4-Dioxane	-	-	274	0.35	331	0.15	390 (sh)

Solvent	I_c						
	A		B		C		D
	λ_{max} (nm)	ε_{max} x 10^4	λ_{max} (nm)	ε_{max} x 10^4	λ_{max} (nm)	ε_{max} x 10^4	λ_{max} (nm)
Ethanol	-	-	242	0.82	317, 293	0.10	364 (sh)
Acetonitril	-	-	234	1.12	293	0.40	370 (sh)
DMF	-	-	-	-	297	0.64	375 (sh)
n-Hexane	-	-	280	0.09	343	0.04	362 (sh)
Acetone	-	-	-	-	340	0.02	360 (sh)
1,4-Dioxane	-	-	-	-	293	0.53	372 (sh)

ε_{max} : (L mol^{-1} cm^{-1})　　　(sh): shoulder

Table (3): *The spectral data of ligands II_{a-c} in different organic solvents*

Solvent	II_a						
	A		B		C		D
	λ_{max} (nm)	$\varepsilon_{max} \times 10^4$	λ_{max} (nm)	$\varepsilon_{max} \times 10^4$	λ_{max} (nm)	$\varepsilon_{max} \times 10^4$	λ_{max} (nm)
Ethanol	230	0.2	277	0.23	330	0.18	397(sh)
Acetonitril	250	0.22	276	0.17	341	0.13	-
DMF	355(sh)	0.28	400(sh)	0.36	436	0.48	-
n-Hexane	243	0.20	-	-	342	0.04	423(sh)
Acetone	-	-	344	0.38	430(sh)	0.29	420(sh)
1,4-Dioxane	-	-	-	-	342	0.64	-
Solvent	**II_b**						
	A		B		C		D
	λ_{max} (nm)	$\varepsilon_{max} \times 10^4$	λ_{max} (nm)	$\varepsilon_{max} \times 10^4$	λ_{max} (nm)	$\varepsilon_{max} \times 10^4$	λ_{max} (nm)
Ethanol	225(sh)	0.52	275	0.36	330	0.30	415 (sh)
Acetonitril	230	0.31	275	0.28	335	0.21	-
DMF	342	0.24	413	0.42	466	0.44	-
n-Hexane	220	0.12	242	0.12	350	0.10	440(sh)
Acetone	-	-	-	-	342	.41	483(sh)
1,4-Dioxane	267	0.50	275(sh)	0.41	344	0.36	485(sh)
Solvent	**II_c**						
	A		B		C		D
	λ_{max} (nm)	$\varepsilon_{max} \times 10^4$	λ_{max} (nm)	$\varepsilon_{max} \times 10^4$	λ_{max} (nm)	$\varepsilon_{max} \times 10^4$	λ_{max} (nm)
Ethanol	-	-	250(sh)	0.71	311	1.36	425(sh)
Acetonitril	-	-	303(sh)	1.00	330	0.80	380(sh)
DMF	-	-	311(sh)	1.11	335	0.60	-
n-Hexane	223	0.17	252	0.08	343	0.04	450(sh)
Acetone	315	1.12	338	0.72	366	0.46	455(sh)
1,4-Dioxane	-	-	308	0.96	340	0.56	453(sh)

ε_{max} : (L mol^{-1} cm^{-1})   (sh): shoulder

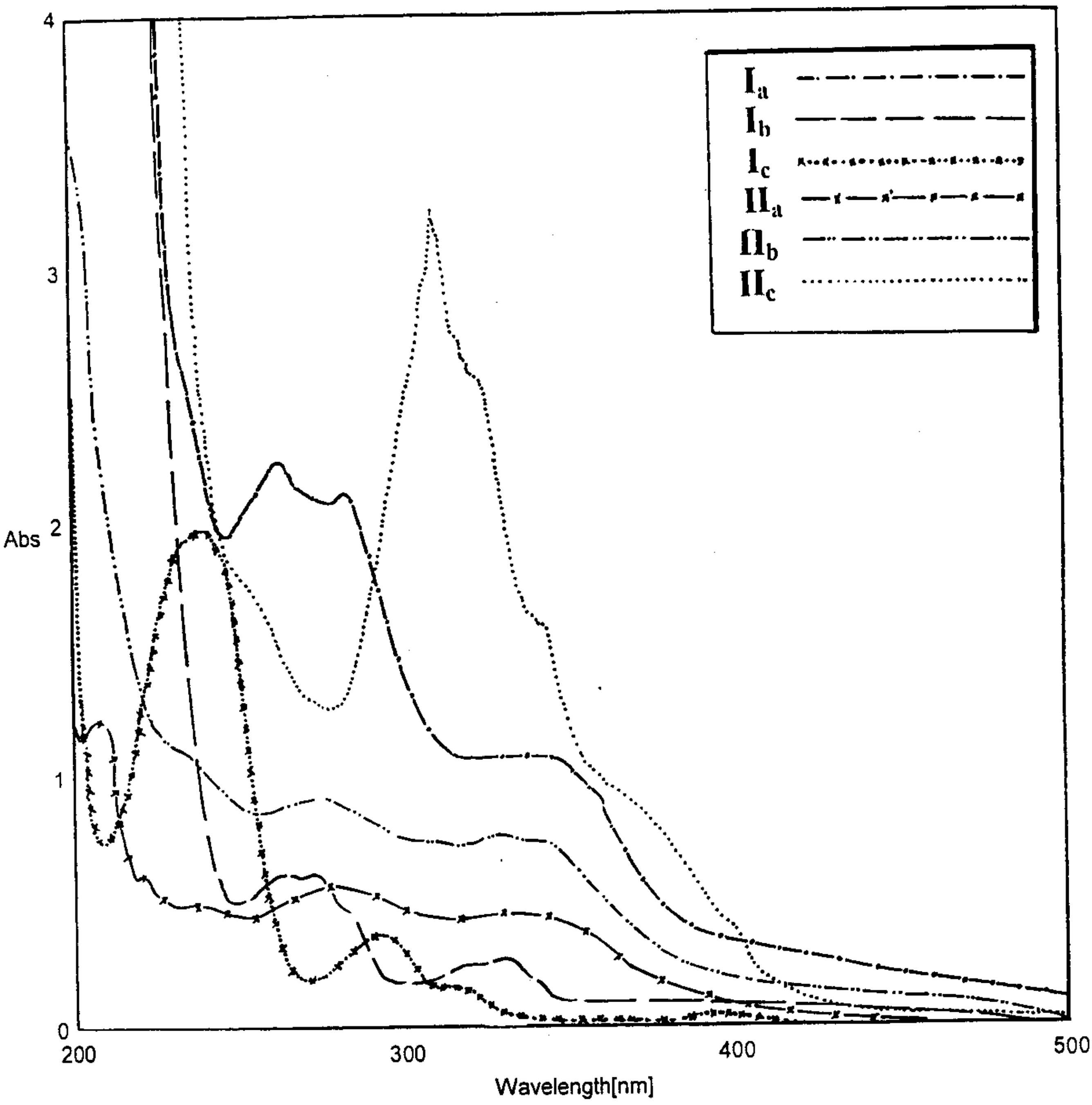

Fig. (2) : *Absorption spectra of all ligands under consideration in ethanol (concentration= 5x10^{-4})*

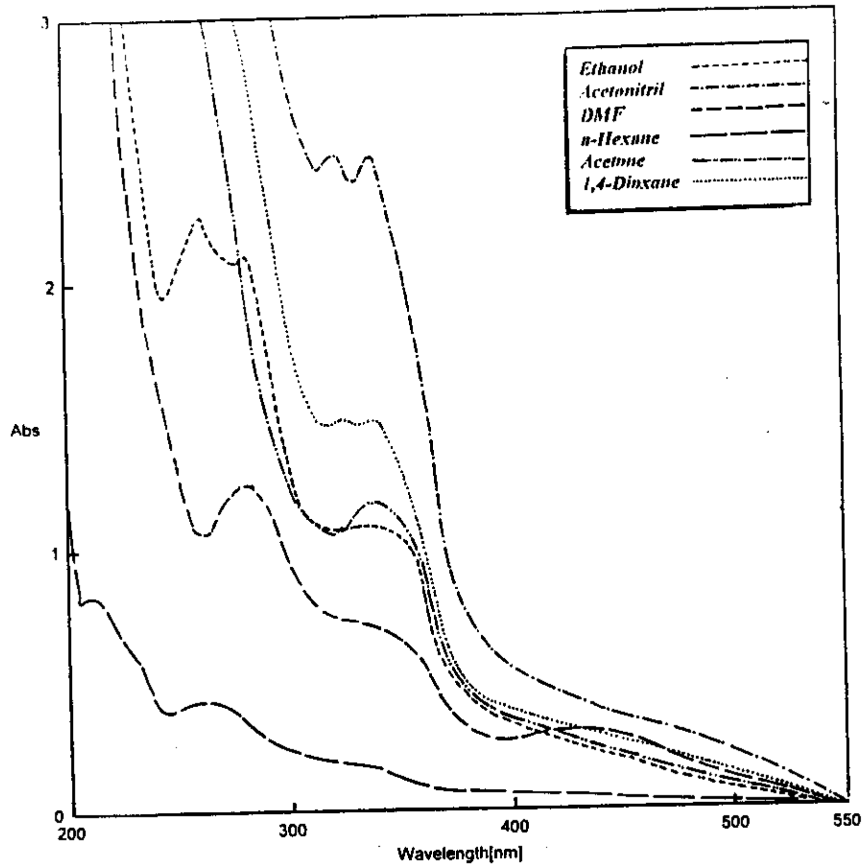

Fig. (3) : *Absorption spectra af 6-(1-Hydroxy-naphthalen-2-ylazo) quinoxaline-2,3-diol (ligand I_a) in different organic solvents (concentration=5 ×10⁻⁴)*

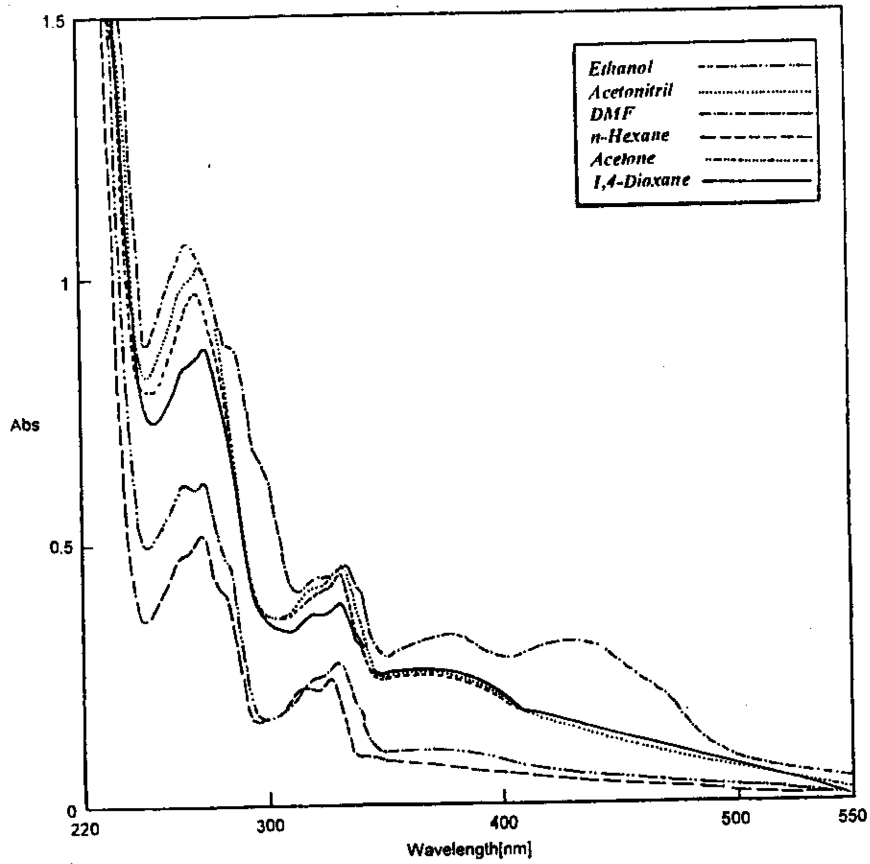

Fig. (4) : *Absorption spectra af 6-(1-Hydroxy-naphthalen -1-ylazo) quinoxaline-2,3-diol (ligand I_b) in different organic solvents (concentrotion=5×10⁻⁴)*

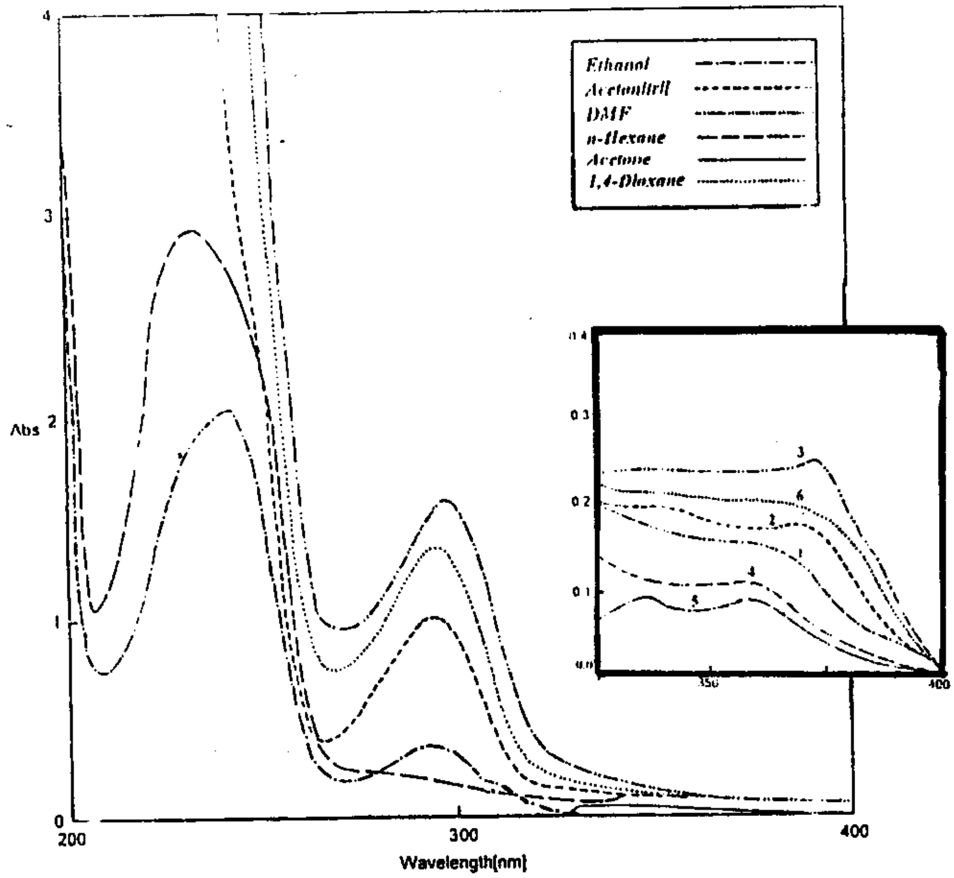

Fig. (5) : *Absorption spectra of 6-(2,5-Dihydroxy-phenylazo) quinoxaline-2,3-diol (ligand I_c) in different organic solvents (concentration=5×10^{-4})*

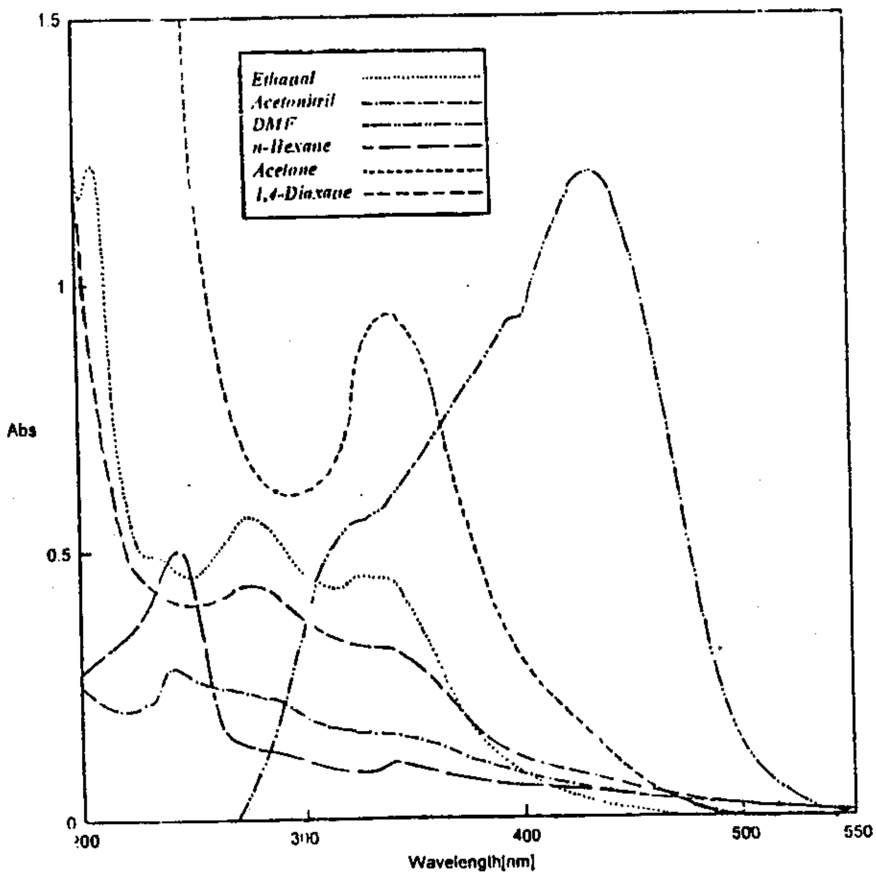

Fig. (6) : *Absorption spectra of 6-[(2-Hydroxy-benzylidene)-amino] quinoxaline-2,3- diol (ligand II_c) in different organic solvents (concentration=5×10^{-4})*

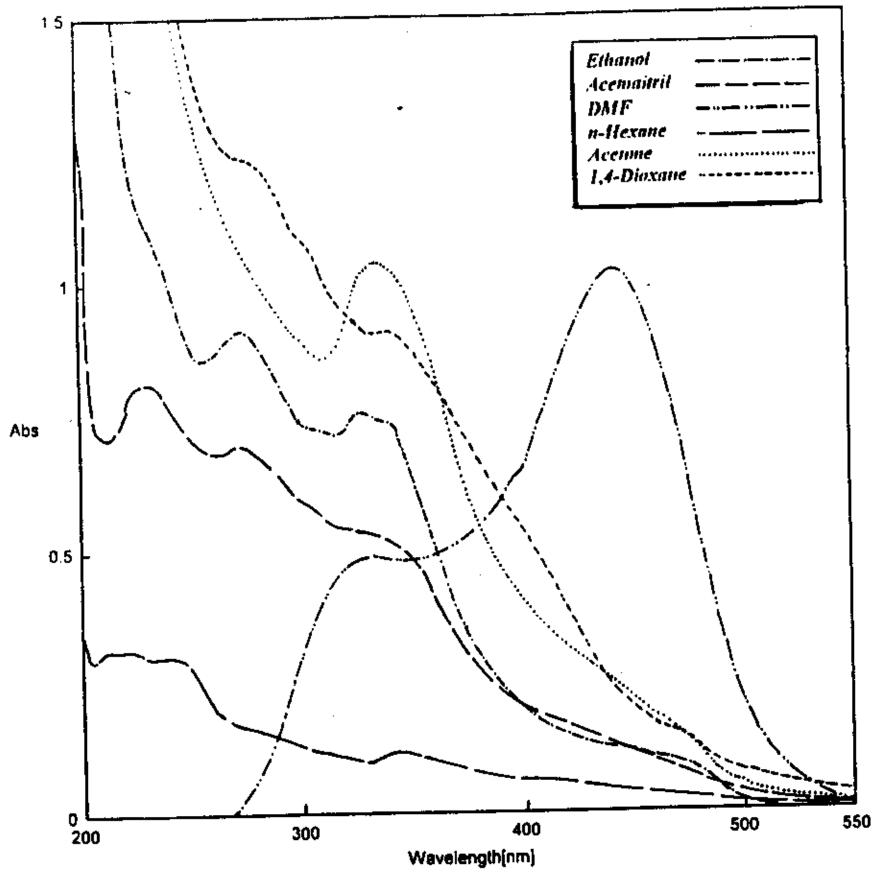

Fig. (7) : *Absorption spectra of 6-{(1-Hydroxy-naphthalen-2-ylmethylene) -amino}quinoxaline-2,3-diol (ligand II_4) in different organic salvents (cancentration=$5*10^{-4}$)*

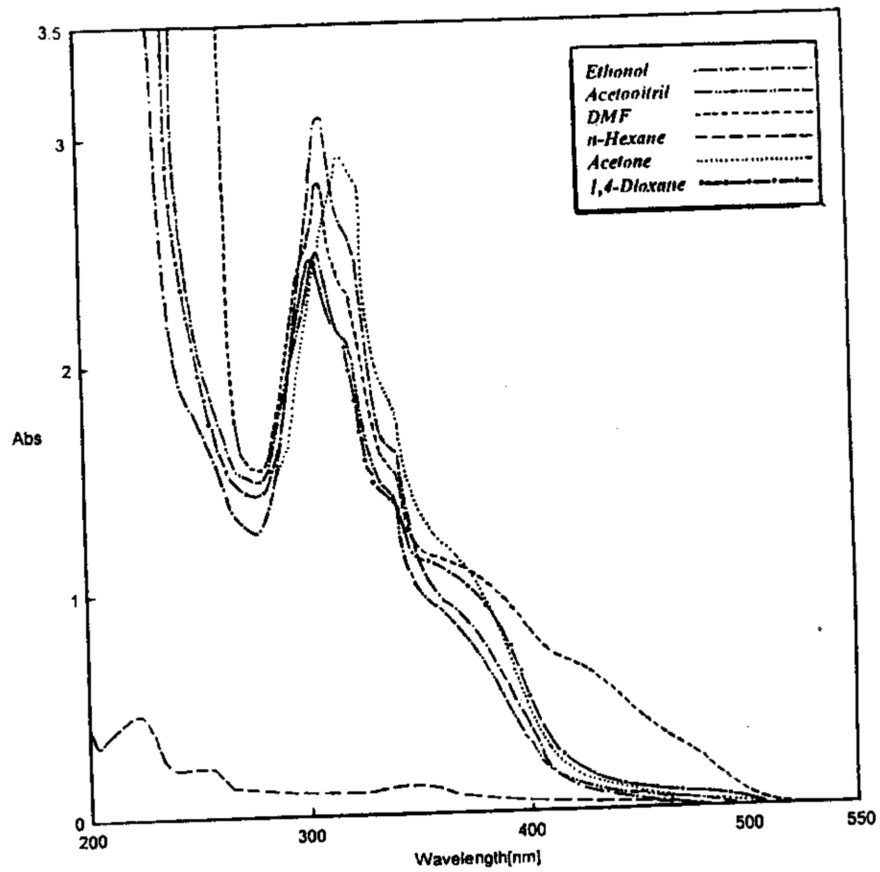

Fig. (8) : *Absorption spectra of 6-{(5-Bromo-2-hydroxy-benzylidene)-amino}quinoxaline-2,3-dial (ligand II_2) in different organic solvents (cancentration=$5*10^{-4}$)*

3.4. The spectral behavior of ligands under consideration in buffer solutions and the determination of their acid ionisation constants

The acid ionization constants (pK_a) of the ligands under investigation are determined specrophotometrically in universal buffer solutions covering the pH range 2.04 to 12.04. The absorption spectra of both azo dyes and Schiff base compounds in buffer solutions of varying pH values are recorded within the wavelength range 250-600 nm. The bands of some compounds were shifted in their position or show variation in extinction whereas others exhibit a new band by increasing pH of the medium as shown in Figs. (9-14). The relation between pH and absorbance of each ligand are shown in Figs. (9-14) which give S-shape and the change of absorbance with pH can be utilized for determination of the dissociation constants by some methods. These include:

1- Half-height method[94]

This method is based on the fact that at the half-height of the absorbance-pH curve, the dissociated and undissociated species exist in equivalent quantities, thus

$$pK = pH \qquad \text{at } A_{1/2}$$

where $A_{1/2} = [(A_{max}-A_{min})/2] + A_{min}$

2- The modified limiting absorbance method[95]

This method has the advantage of eliminating any overlaps between absorbance of the two forms, and pK_a is calculated by equation

$$pH = pK + \log \gamma' + \log [(A-A_{min})/(A_{max} - A)]$$

where

A = absorbance at a given pH value

γ = the activity coefficient of the ion present at equilibrium

A_{min}, A_{max} are the absorbance corresponding to the total concentration of neutral and ionized species liable to exist in solution.

The pK_a value can be evaluated by plotting log $[(A-A_{min})/(A_{max}-A)]$ vs pH. The pK_a value thus corresponds to the pH value at zero log $[(A-A_{min})/(A_{max}-A)]$.

3- The colleter method [96]

This method is utilized in the form developed for the determination of the dissociation constants of weak acids. In this method, three absorbance values are taken at three different hydrogen ion concentration at the same wavelength.

The dissociation constants can be calculated using the following equations

$$K_a = \frac{C_{H_2^+} - MC_{H_3^+}}{M-1}$$

in which

$$M = \left(\frac{A_3 - A_1}{A_2 - A_1}\right) \cdot \left(\frac{C_{H_1^+} - C_{H_2^+}}{C_{H_1^+} - C_{H_3^+}}\right)$$

Where A_1, A_2, A_3 are the absorbance at three different H^+ ion concentration $C_{H_1^+}$, $C_{H_2^+}$ and $C_{H_3^+}$ respectively

The pK_a values determined by the different methods for the reagents I_{a-c} and II_{a-c} are given in Table (12).

3.4.1. The spectra of ligands I_a, I_b, and I_c in universal buffer solutions

The spectra of 1 x 10^{-5} M of azo compounds I_a, I_b and I_c in buffer solutions containing 30 % (v/v) ethanol of pH 2.04-12.04 are shown in Figs. (9-11).

The spectra of I_a and I_b show one band is λ_{max} 420 and 390 nm respectively which increased in extinction with increasing the pH of the medium. But in case of I_c, the spectra show two bands of λ_{max} 388 and 483 nm where band at 388 nm increased in extinction with increasing the pH of the medium, but band at 483 nm decreased in extinction with increasing pH value. A clear isosbestic point for I_c appeared at 455 nm, which indicates that an acid-base equilibrium occurred between the non-ionized and ionized species; this can be represented as follows:

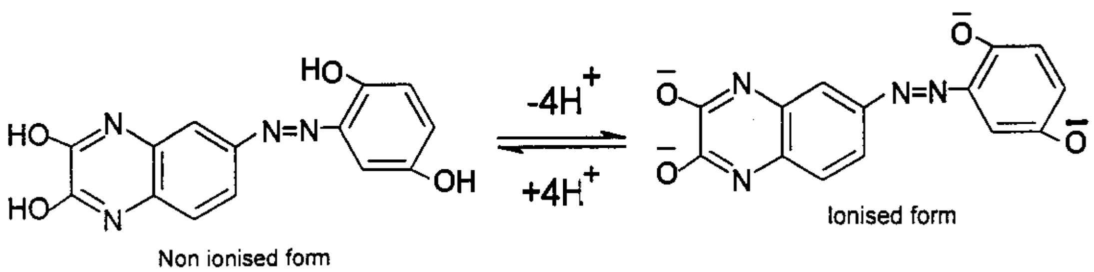

The variation of absorbance with pH for I_a, I_b and I_c at λ_{max} gives S-shaped curves as shown in Figs (9-11) and data given in Tables (4-7).

3.4.2. The absorption spectra of ligands II_a, II_b and II_c in universal buffer solutions

The absorption spectra of 1 x 10^{-5} M of Schiff-base compounds II_a, II_b and II_c in buffer solutions containing 30% (v/v) ethanol are shown in Figs. (12-14). It is clear that the absorption of the species changes with increase of pH of medium.

In case of II_a the spectra show one band at λ_{max} = 398 nm with a shoulder at longer wavelength, which developed to a band at λ_{max} = 478 nm with increasing pH values. In case of II_b and II_c only one band appears with λ_{max} of 410 and 394 nm respectively which increased in extinction with increasing the pH of the medium. A clear isosbestic point for II_a appears at 425 nm, which indicates that an acid-base equilibrium occurred between the non-ionized and ionized species occurs in solutions; this may be represented as follows:

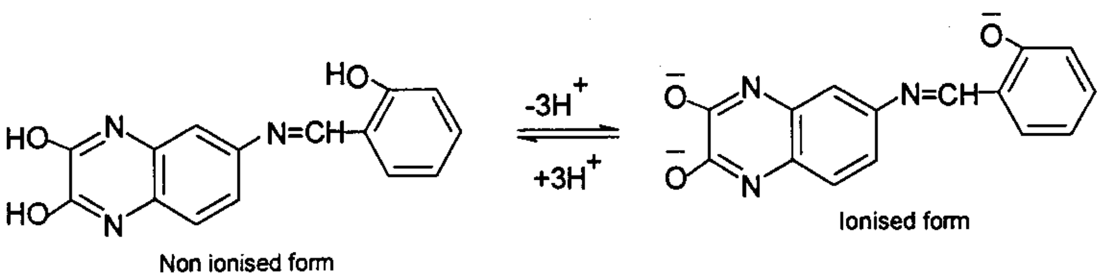

The variation of absorbance with pH of solution for compounds II_a, II_b and II_c are given in Figs. (9-11) as S-shape with one or two inflection and data are given in Tables (4-7). The inflections lie within the pH ranges 3.2-6.4 and 7.1-10.5 revealing that the ionization of the two OH groups occurs in a stepwise manner.

Table (4). ***The colleter method of ligand I_a at λ_{max} = 420 nm***

Points	p H	A	Point taken	M	K_a	pK_a
1	2	0.022	2, 3, 5	13.500	7.89×10^{-6}	5.10
2	3	0.025	1, 4, 6	4.500	8.28×10^{-7}	6.08
3	4	0.030	2, 4, 6	4.980	7.40×10^{-7}	6.13
4	5.5	0.050	3, 5, 7	1.140	3.05×10^{-8}	7.51
5	7	0.100	7, 8, 9	6.820	5.46×10^{-12}	11.26
6	8	0.150	8, 9, 10	4.160	8.20×10^{-9}	8.08
7	9	0.320	4, 6, 8	2.990	4.87×10^{-9}	8.31
8	10	0.350	1, 7, 8	1.100	8.84×10^{-9}	8.05
9	11	0.545	5, 9, 10	1.033	2.70×10^{-10}	9.56
10	12	0.560	3, 7, 9	1.741	1.26×10^{-9}	8.89
Mean pK_a = 7.89						

Table (5). ***The colleter method of ligand I_b at λ_{max} = 390nm***

Points	p H	A	Point taken	M	K_a	pK_a
1	2	0.07	2, 4, 5	1.370	7.71×10^{-6}	5.11
2	3	0.08	2, 5, 7	1.820	1.20×10^{-7}	6.92
3	4	0.09	3, 7, 9	1.325	3.13×10^{-9}	8.51
4	5.5	0.16	2, 6, 8	1.920	1.07×10^{-8}	7.97
5	7	0.19	4, 7, 9	1.499	1.97×10^{-9}	8.70
6	8	0.20	1, 5, 9	2.250	2.82×10^{-10}	9.10
7	9	0.28	3, 6, 8	1.990	9.80×10^{-9}	8.00
8	10	0.32	1, 8, 10	1.320	3.08×10^{-10}	9.51
9	11	0.34	1, 6, 9	1.990	9.98×10^{-9}	8.00
10	12	0.40	5, 7, 9	1.650	1.52×10^{-9}	8.22
Mean pK_a = 8.00						

Table (8). ***The colleter method of ligand II_a at λ_{max} = 398nm***

Points	p H	A	Point taken	M	K_a	pK_a
1	2	0.095	2, 4, 6	2.80	1.64×10^{-6}	5.78
2	3	0.110	1, 3, 5	4.13	3.17×10^{-5}	4.49
3	4	0.180	2, 5, 7	1.17	5.61×10^{-7}	6.25
4	5.5	0.245	3, 5, 6	1.15	6.01×10^{-7}	6.22
5	7	0.450	4, 5, 7	1.46	2.12×10^{-7}	6.67
6	8	0.490	1, 5, 7	1.17	5.80×10^{-7}	6.23
7	9	0.510	2, 3, 6	4.88	2.50×10^{-5}	4.59
Mean pK_a = 5.75						

Table (9). ***The colleter method of ligand II_a at λ_{max} = 478nm***

Points	p H	A	Point taken	M	K_a	pK_a
1	2	0.025	3, 6, 9	6.19	1.92×10^{-6}	8.71
2	3	0.030	2, 4, 6	4.89	7.40×10^{-7}	6.13
3	4	0.035	3, 5, 7	4.99	2.49×10^{-8}	7.60
4	5.5	0.036	1, 4, 6	3.18	1.36×10^{-6}	5.86
5	7	0.050	5, 7, 9	2.33	7.33×10^{-11}	10.13
6	8	0.060	4, 6, 8	5.58	2.17×10^{-9}	8.66
7	9	0.110	3, 7, 9	2.06	9.18×10^{-11}	10.03
8	10	0.170	2, 6, 9	4.66	2.70×10^{-9}	8.56
9	11	0.190	3, 7, 8	1.79	1.03×10^{-10}	9.98
Mean pK_a = 8.41						

Table (10). ***The colleter method of ligand II_b at $\lambda_{max} = 410nm$***

Points	p H	A	Point taken	M	K_a	pK_a
1	2	0.070	1, 4, 7	5.23	7.08×10^{-7}	6.15
2	3	0.090	2, 4, 8	6.16	5.81×10^{-7}	6.23
3	4	0.095	4, 6, 8	1.89	1.09×10^{-8}	7.90
4	5.5	0.200	5, 7, 9	1.09	1.09×10^{-8}	7.95
5	7	0.260	1, 7, 8	1.03	3.05×10^{-8}	7.51
6	8	0.500	4, 7, 10	1.11	9.18×10^{-9}	8.04
7	9	0.750	3, 5, 9	4.27	3.05×10^{-8}	7.51
8	10	0.770	4, 8, 10	1.07	1.41×10^{-9}	8.85
9	11	0.800	2, 8, 9	1.04	2.26×10^{-11}	11.35
10	12	0.810	1, 3, 9	28.90	3.58×10^{-6}	5.44
Mean $pK_a = 7.69$						

Table (11). ***The colleter method of ligand II_c at $\lambda_{max} = 394nm$***

Points	p H	A	Point taken	M	K_a	pK_a
1	2	0.075	3, 7, 10	2.03	9.65×10^{-10}	9.01
2	3	0.090	2, 6, 8	2.18	8.27×10^{-9}	8.08
3	4	0.095	1, 4, 6	1.66	8.48×10^{-6}	5.35
4	5.5	0.150	2, 8, 10	1.29	3.38×10^{-10}	9.47
5	7	0.195	1, 5, 7	1.42	3.36×10^{-7}	6.63
6	8	0.200	3, 6, 10	2.90	5.25×10^{-9}	8.27
7	9	0.245	4, 8, 9	1.16	5.30×10^{-10}	9.27
8	10	0.330	5, 6, 10	36.90	2.77×10^{-10}	9.55
9	11	0.390	3, 5, 7	1.49	1.97×10^{-7}	6.70
10	12	0.400	1, 7, 9	2.60	5.25×10^{-9}	8.27
Mean $pK_a = 8.06$						

Table (12). ***The ionization constants (pK_a) for azo dye and Schiff-base compounds***

Ligand	Ionization constant	pK_a			Average
		1	2	3	
I_a	pK_{a1}	10.61	9.95	7.89	9.48
	pK_{a2}	8.21	----	----	8.21
	pK_{a3}	6.00	----	----	6.00
I_b	pK_{a1}	8.95	8.61	8.00	8.52
	pK_{a2}	-----	7.70	----	7.70
	pK_{a3}	4.85	----	----	4.85
I_c	pK_{a1}	9.53	9.35	----	9.44
	pK_{a2}	----	9.21	8.44	8.83
	pK_{a3}	6.64	6.22	6.22	6.23
	pK_{a4}	4.91	----	----	4.91
II_a	pK_{a1}	9.83	9.59	8.41	9.28
	pK_{a2}	6.31	5.00	5.75	5.69
	pK_{a3}	4.01	----	----	4.01
II_b	pK_{a1}	----	9.82	----	9.82
	pK_{a2}	8.01	7.93	7.69	7.87
	pK_{a3}	5.22	----	----	5.22
II_c	pK_{a1}	9.03	8.95	----	8.99
	pK_{a2}	----	8.02	8.06	8.04
	pK_{a3}	5.25	----	----	5.25

(1) The half-height method.
(2) The modified limiting method.
(3) The colleter method.

Absorbance spectra of ligand (I_a) in buffer solutions

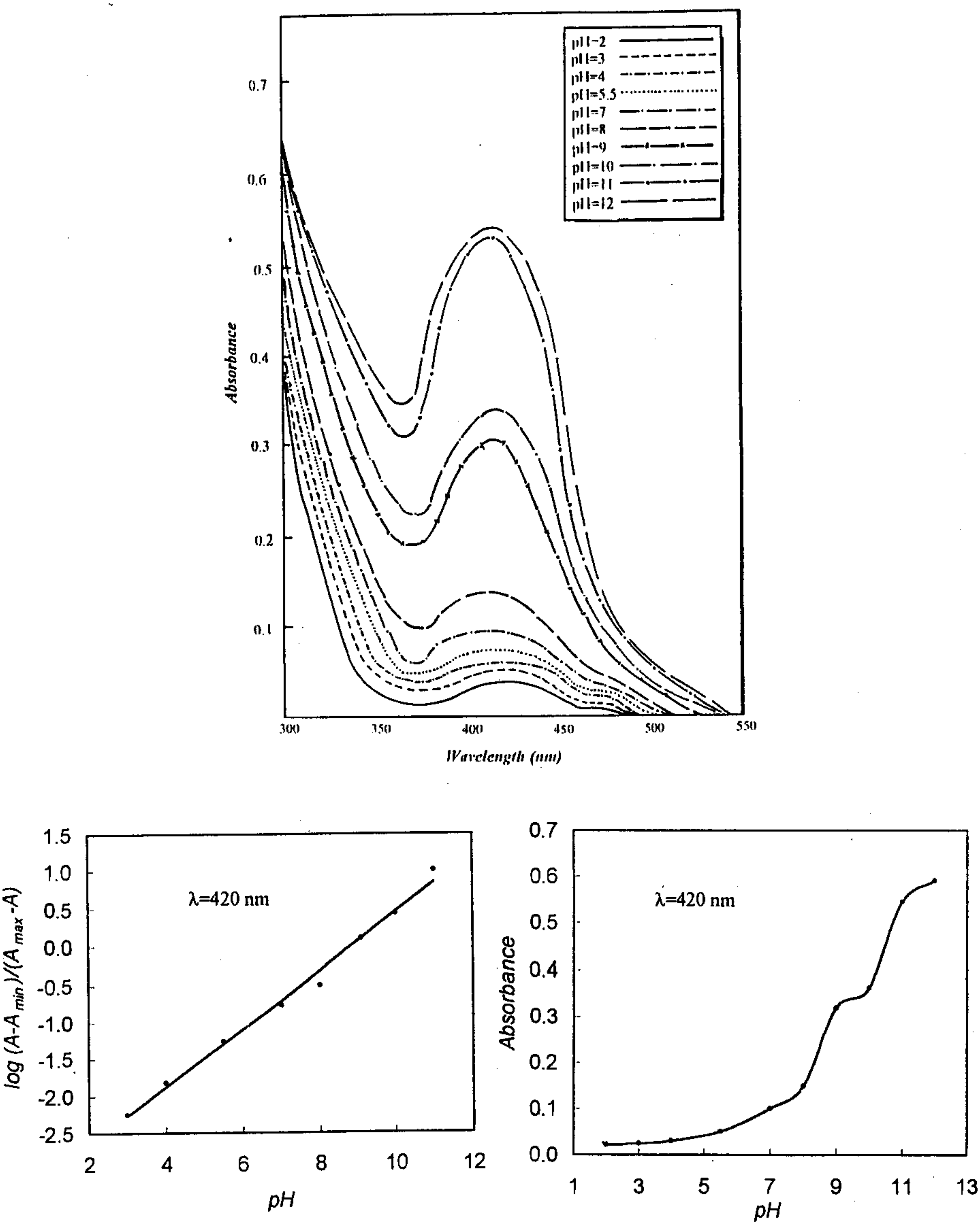

Fig. (9)

Absorbance spectra of ligand (I_b) in buffer solutions

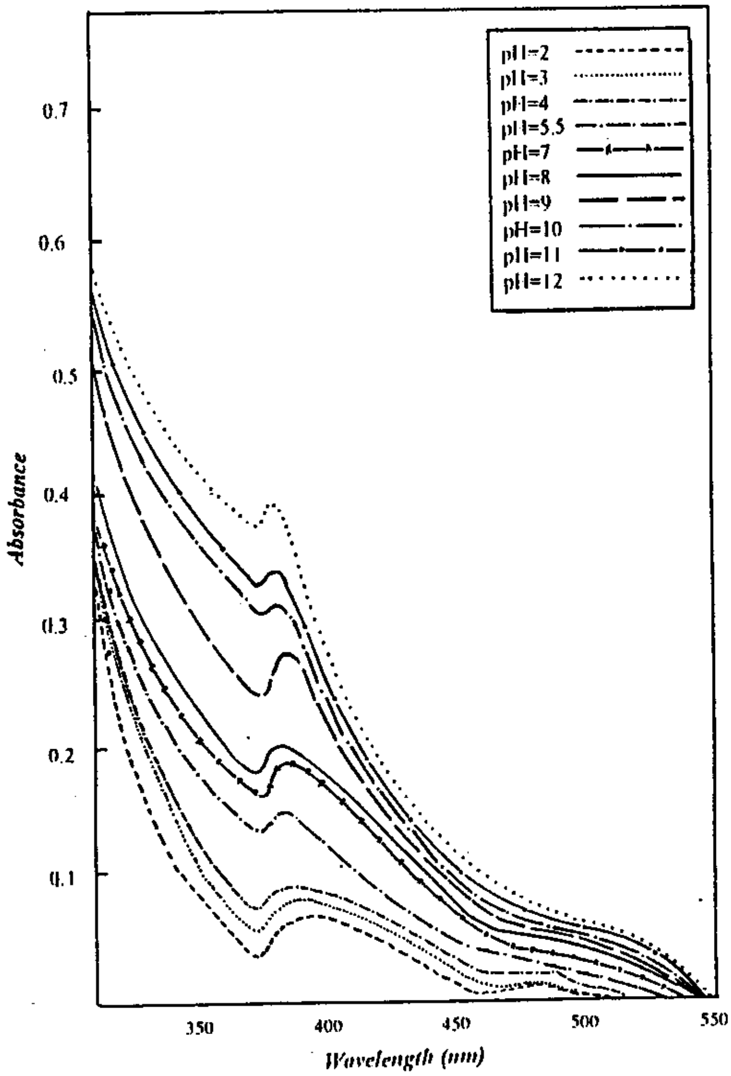

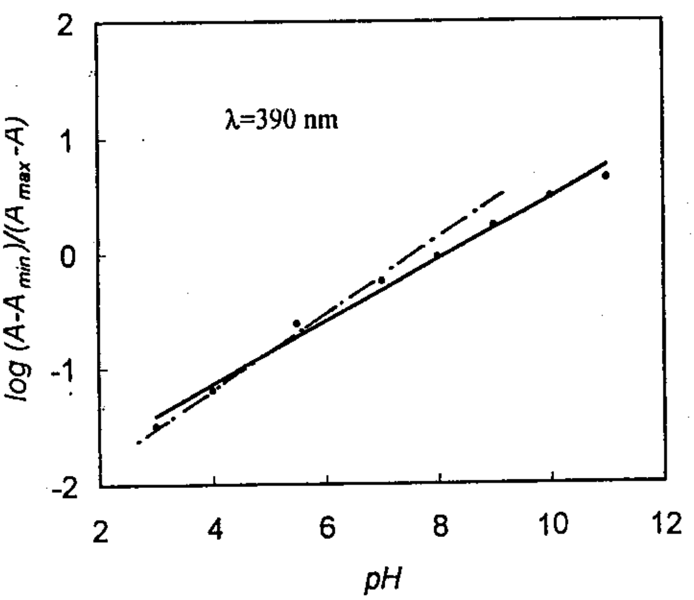

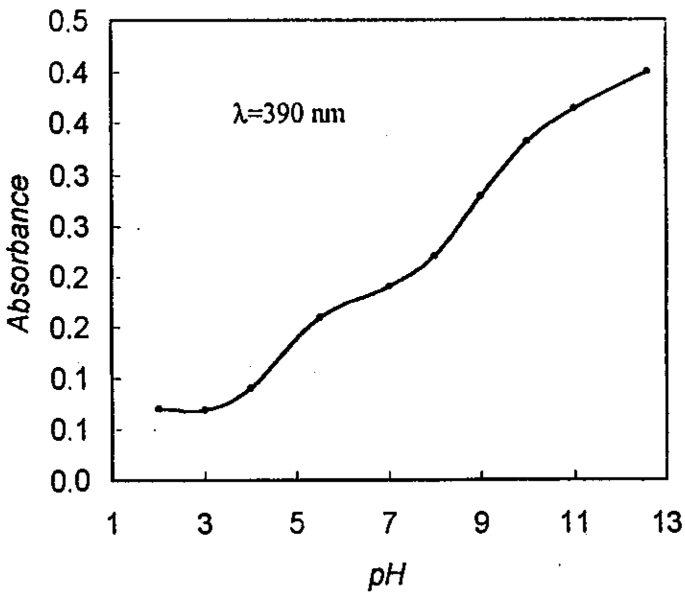

Fig. (10)

Absorbance spectra of ligand (I_c) in buffer solutions

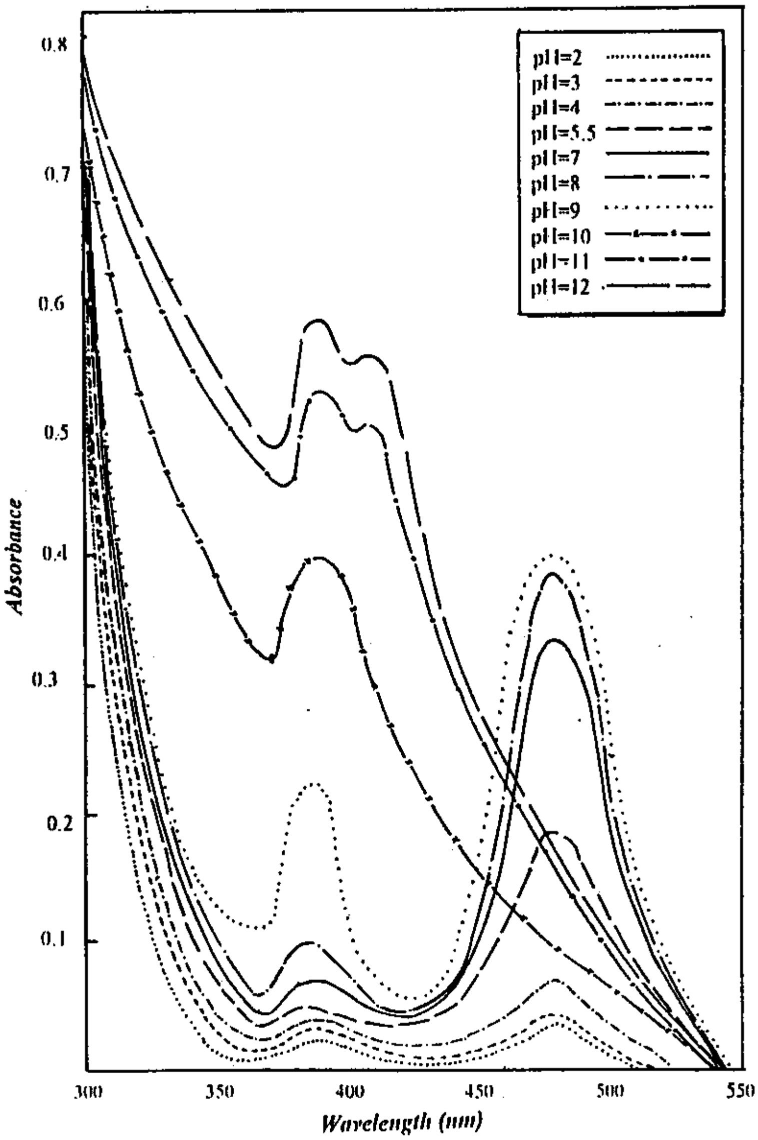

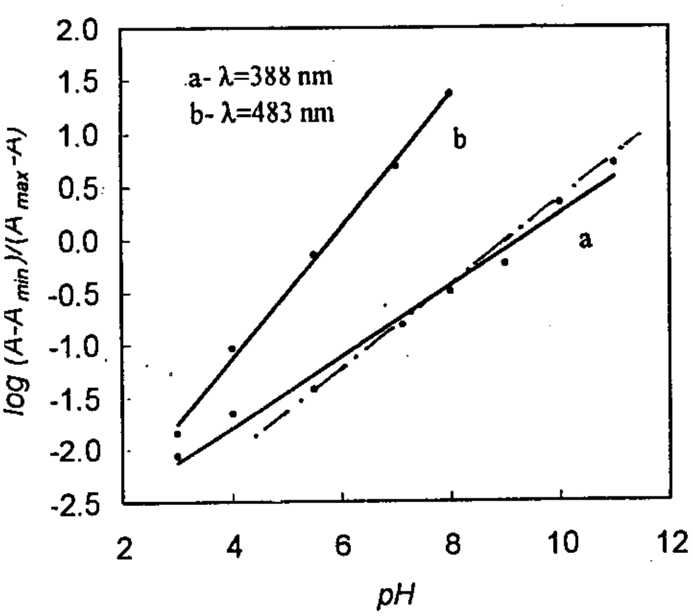

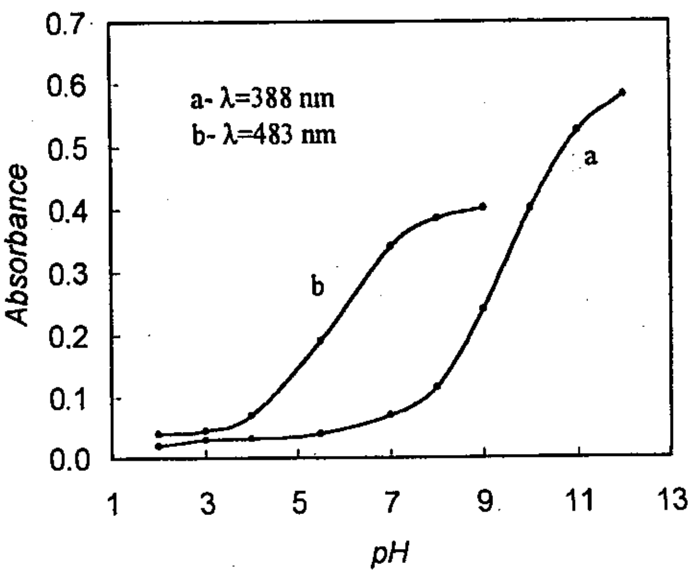

Fig. (11)

Absorbance spectra of ligand (II_a) in buffer solutions

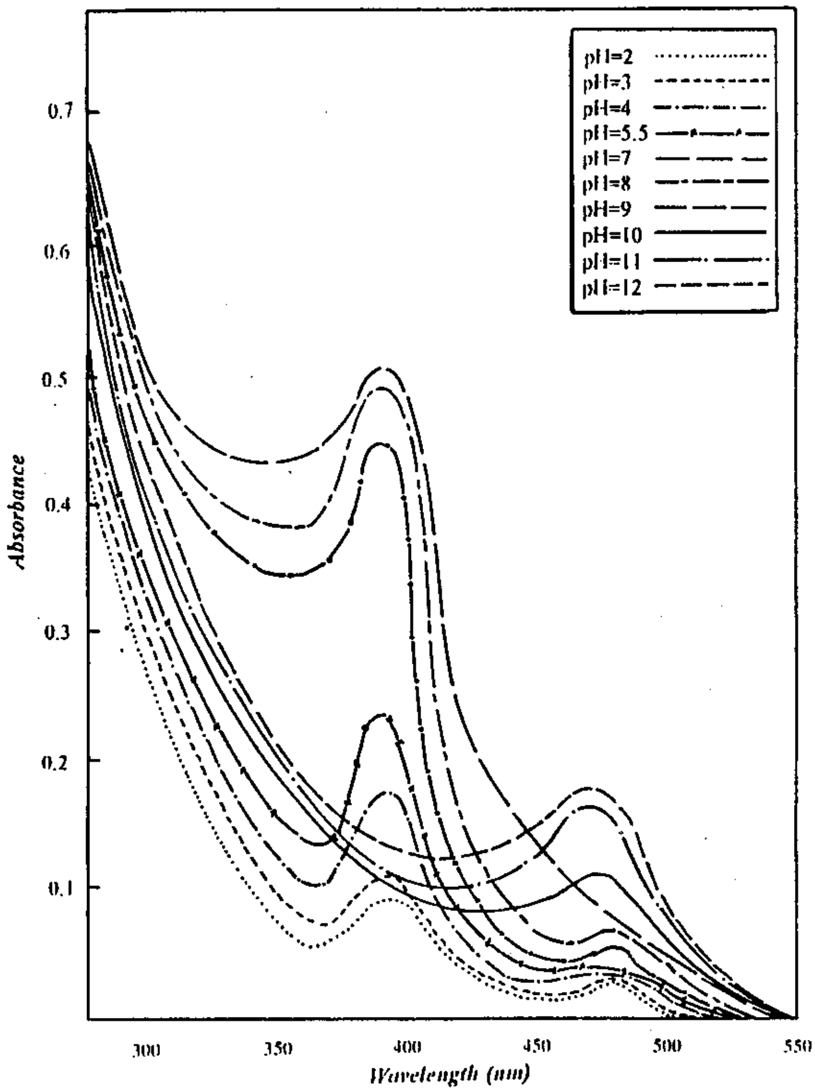

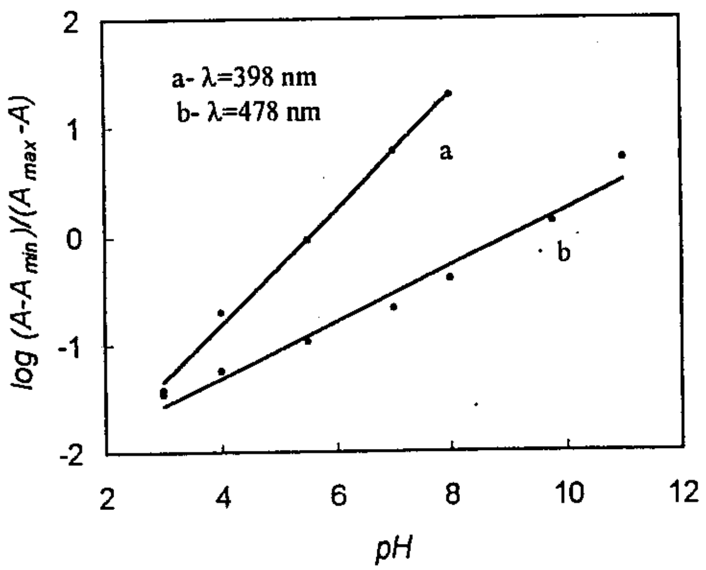

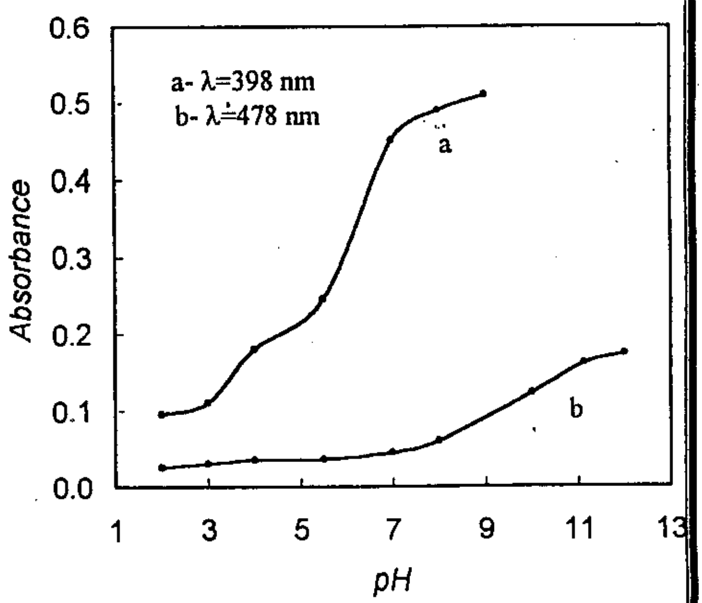

Fig. (12)

Absorbance spectra of ligand (II_b) in buffer solutions

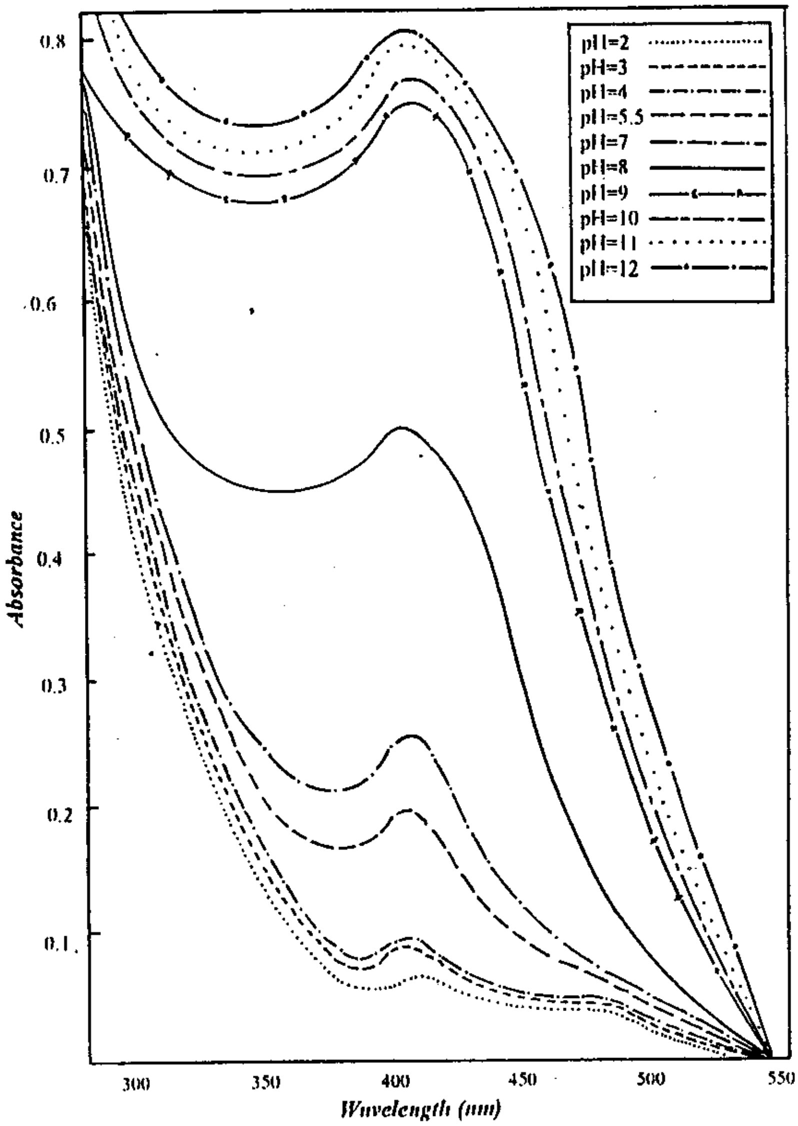

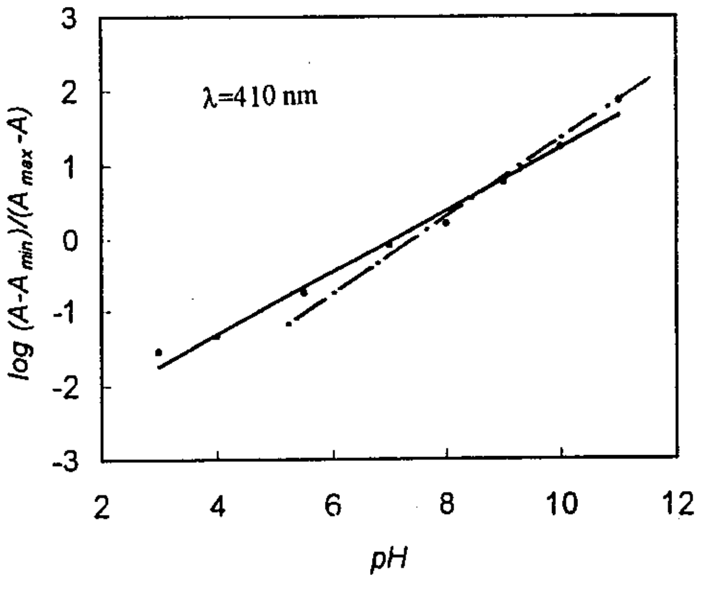

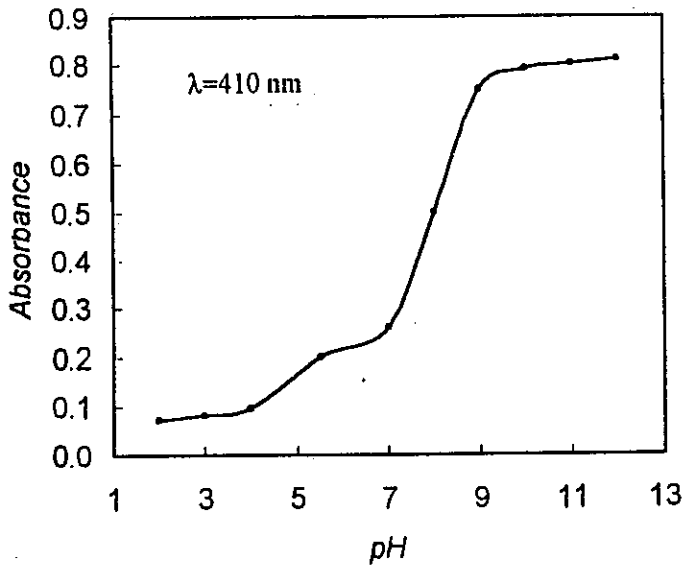

Fig. (13)

3.5. Infrared spectra of free azo dye and Schiff base compounds

This part includes an attempt to obtain the assignment for the important and characteristic bands in the IR-spectra of the reagent under investigation. The IR-spectra of the azo dye and Schiff base compounds under investigation are recorded in Figs. (15-17). The assignment of the important bands is given in Tables (52-57).

3.5.1. Infrared spectra of azo dye compounds

In region of 3500-3300 cm^{-1}, the bands due to the (OH) stretching vibrations are expected to appear. For the first series of compounds (I_{a-c}), the ν_{OH} band appears as a sharp absorption with medium intensity at frequency of 3450, 3453 and 3413 cm^{-1} for I_a, I_b and I_c respectively.

The ν_{C-H} band for aromatic system appears at 3010, 3022 and 3015 cm^{-1} for ligand I_a, I_b and I_c respectively. The C=C band appears at 1670, 1620 and 1510 cm^{-1} for I_a, I_b and I_c respectively.

The spectra in range 1600-1000 cm^{-1} of the azo dye compounds is of interest, since the bands observed are for $\nu_{C=N}$, $\nu_{N=N}$ and ν_{C-O} vibrations. The IR spectra of compounds I_{a-c} show medium or weak intensity bands at 1440, 1458 and 1465 cm^{-1} for ligand I_a, I_b and I_c respectively due to the symmetric vibration of N=N group.

The $\nu_{C=N}$ band is observed at 1565, 1545 and 1505 cm^{-1} for ligand I_a, I_b and I_c respectively. The appearance of the $\nu_{C=N}$ band for these compounds gives an indication that azo $\rightleftharpoons$ hydrazo equilibrium is liable to take place which can be represented as follows:

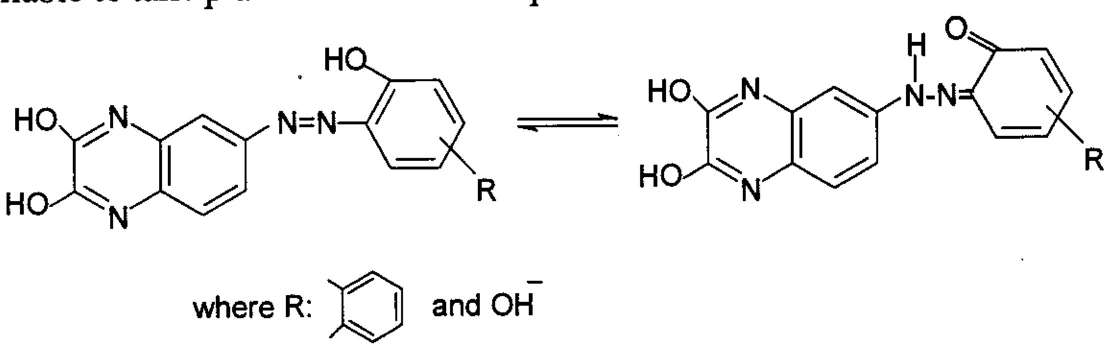

The position of $\nu_{C=O}$ in this case appear at 1630, 1644 and 1620 cm^{-1} for ligands I_a, I_b and I_c respectively. In the spectra of range 1000-400 cm^{-1}, most of strong bands appear in this region in the spectra of azo dyes under investigation which are attributed to the out of plane deformation vibration of the aromatic C-H bonds. The IR spectra of all compounds show a strong band in region 800-550 cm^{-1} corresponding the out of plane of the aromatic hydrogen atom.

The bands around 1380-1330 cm^{-1} are corresponding to the in-plane bending modes of OH group. Also, a band is observed around 1158-1220 cm^{-1} corresponding to the stretching vibration of C-OH and that around 1500-1580 cm^{-1} for stretching vibration of C=N bonds.

3.5.2. Infared spectra of Schiff base compounds

For ligands $II_{a\text{-}c}$ and in region 3500-3300 cm^{-1}, the bands due to the (OH) stretching vibration appeared at 3420, 3433 and 3490 cm^{-1} for II_a, II_b and II_c respectively. The in-plane bending modes of OH group appeared at 1345, 1343 and 1385 cm^{-1} for ligand II_a, II_b and II_c respectively. The $\nu_{C=C}$ band appears at 1610, 1612 and 1615 cm^{-1} for ligands II_a, II_b and II_c respectively.

The aromatic C-H stretching vibrations bands occur in reagion 3080-3010 cm^{-1} and are of strong to medium intentisty where its appear at 3065, 3050 and 3020 cm^{-1} for ligand II_a, II_b and II_c respectively.

The spectra in range 1700-1200 cm^{-1} of Schiff base compounds show bands due to $\nu_{C\text{-}O}$ and $\nu_{sy\ C=N}$ where the symmetric vibrations of C=N group for Schiff base ligands at 1681, 1683 and 1690 cm^{-1} for II_a, II_b and II_c respectively and $\nu_{C\text{-}OH}$ appeared at 1221, 1227 and 1161 cm^{-1} for II_a, II_b and II_c respectively.

Infrared spectra of reagents under consideration

I_a

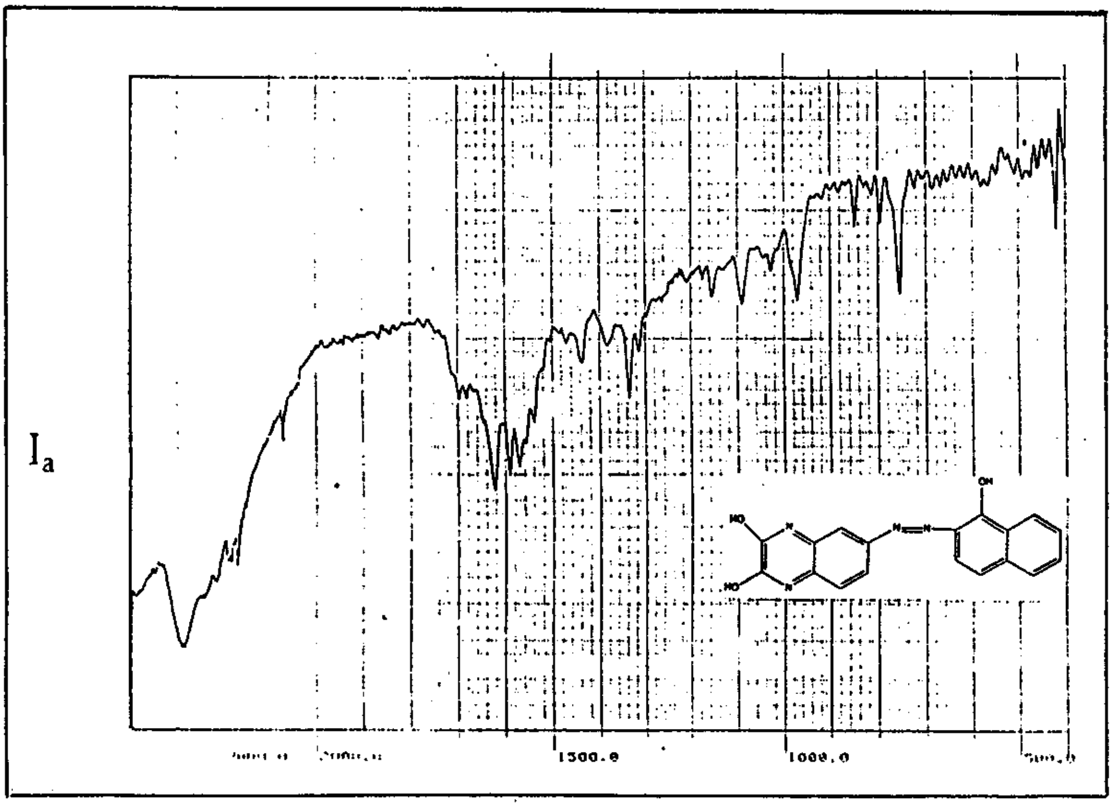

I_b

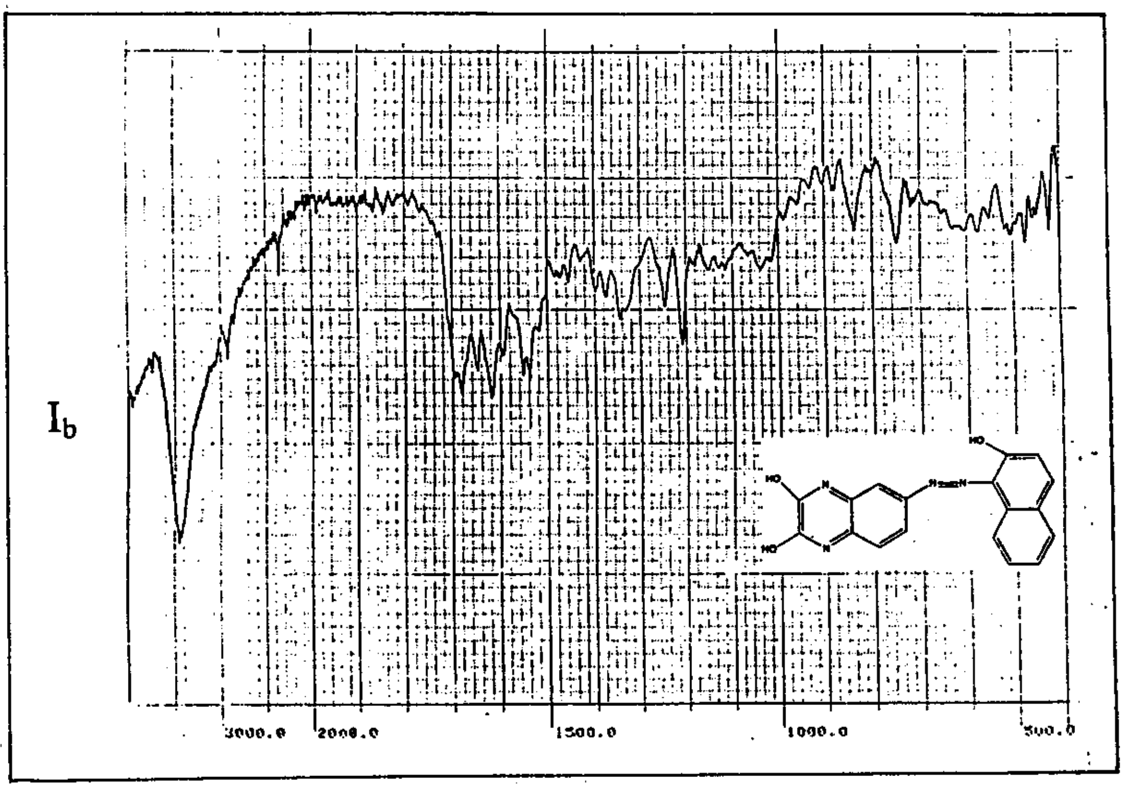

Fig. (15)

Infrared spectra of reagents under consideration

I$_c$

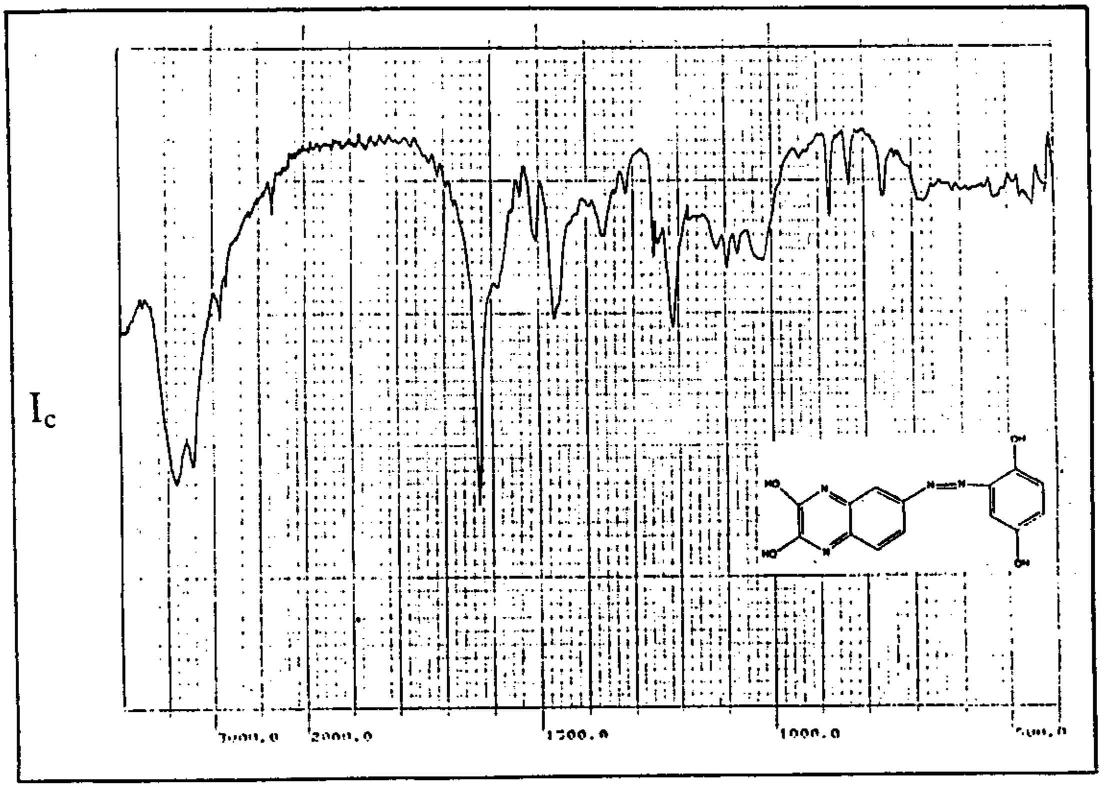

II$_a$

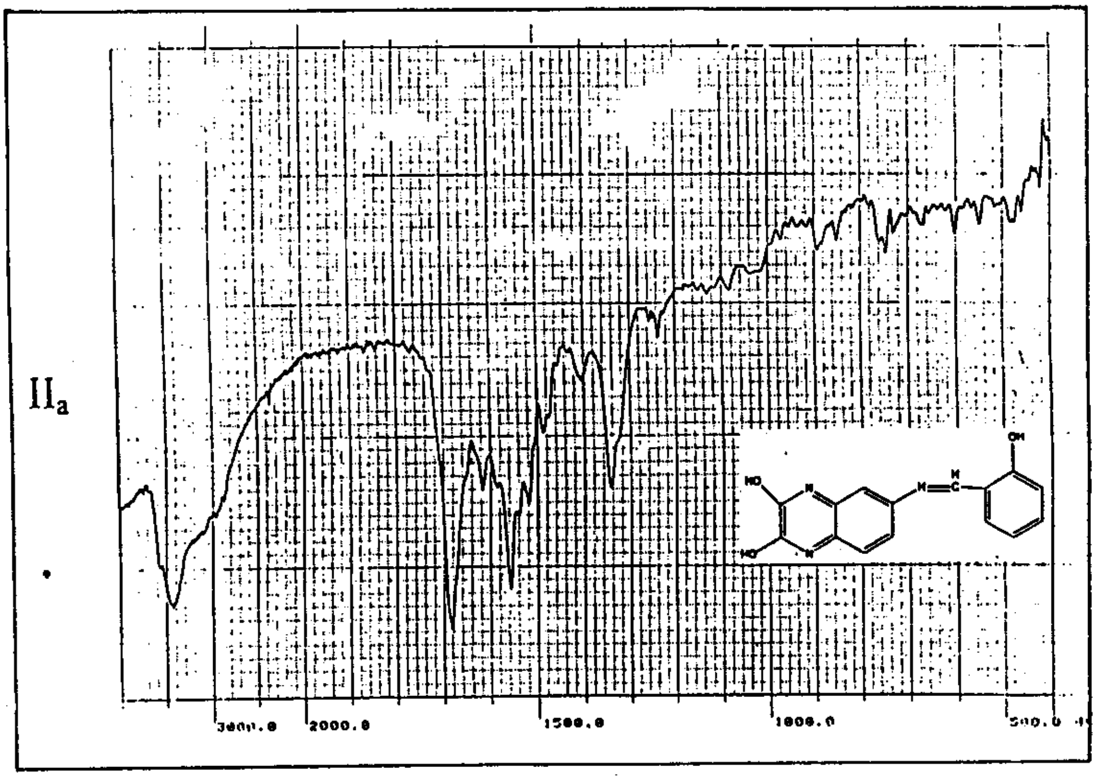

Fig. (16)

Infrared spectra of reagents under consideration

II_b

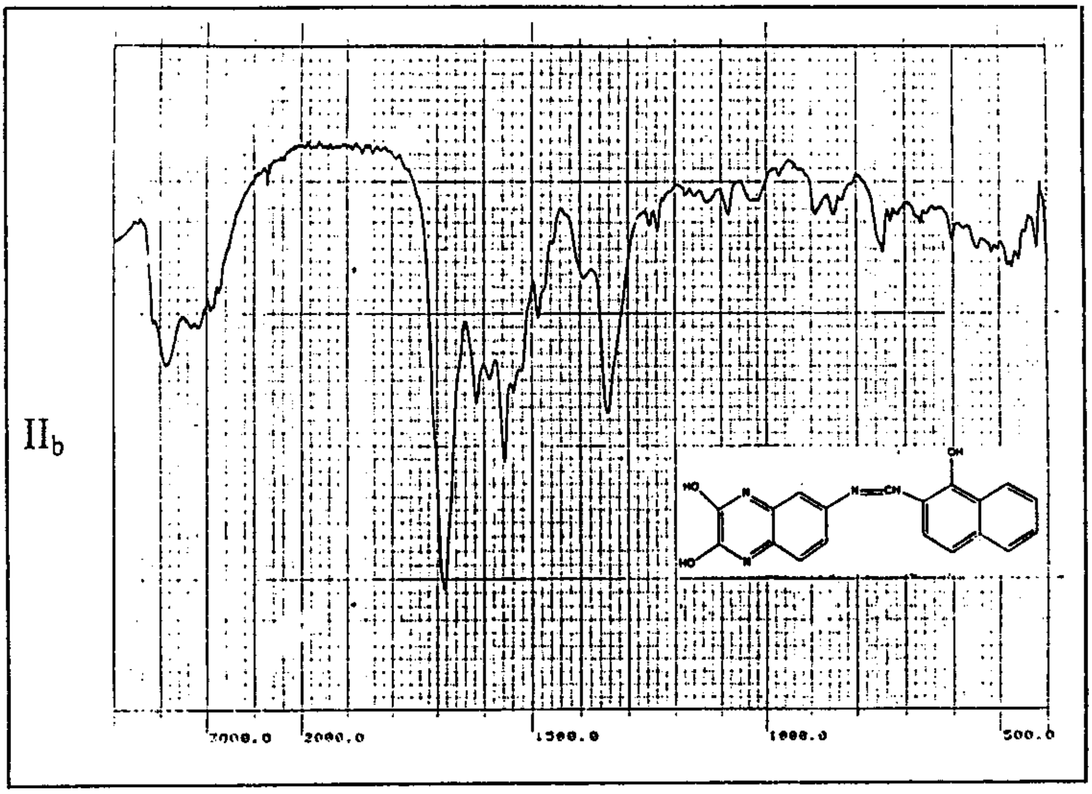

II_c

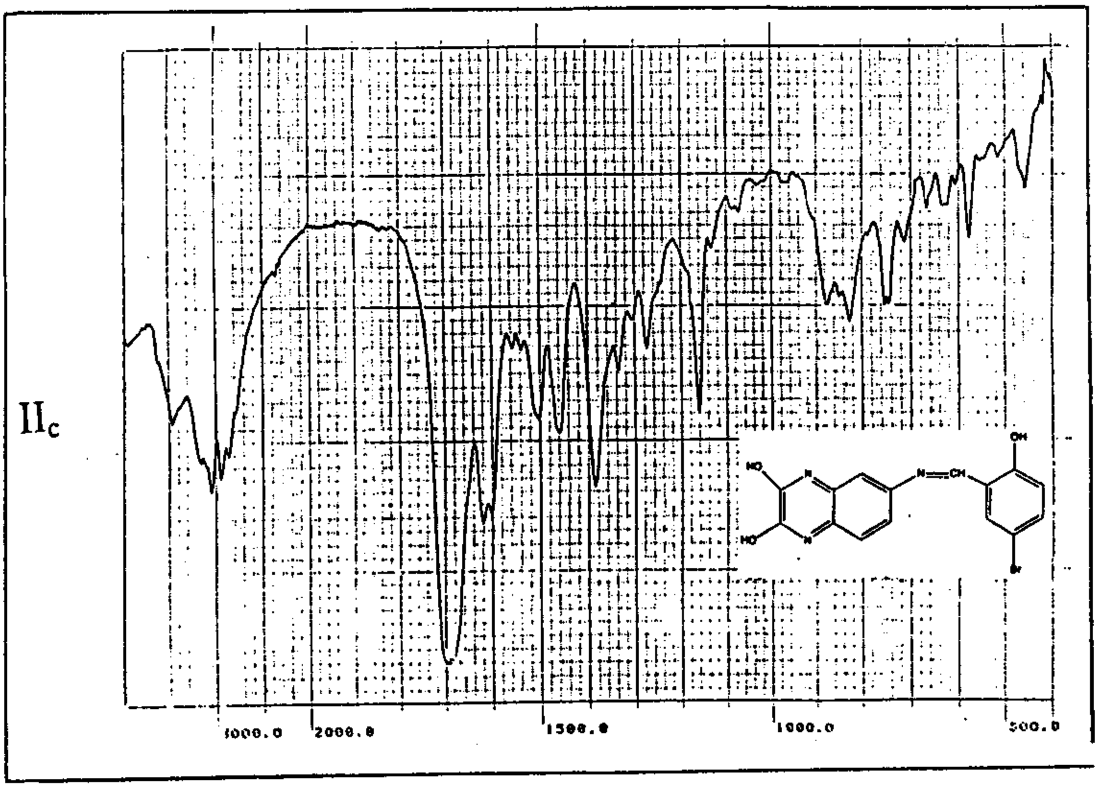

Fig. (17)

3.6. ^{1}H-NMR spectra of ligands under consideration

A further support for the conclusion obtained from elemental analysis and IR spectra for the structure of ligands under investigation is gained by a consideration of their ^{1}H-NMR spectra. The different types of hydrogen protons which are expected for the compounds under investigation can be formulated as follows:

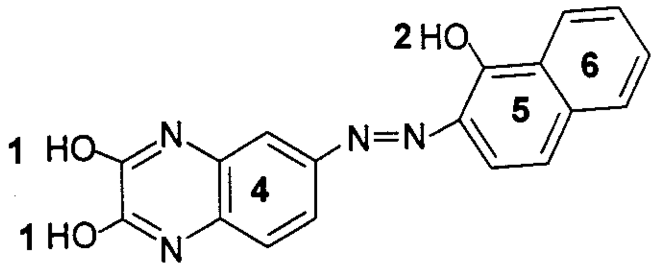

I_a

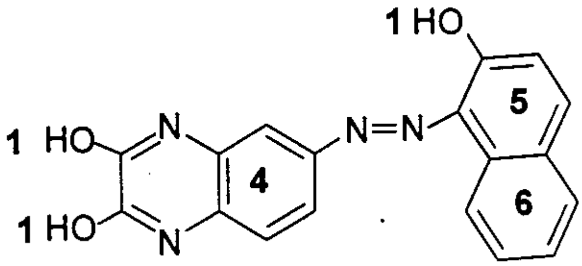

I_b

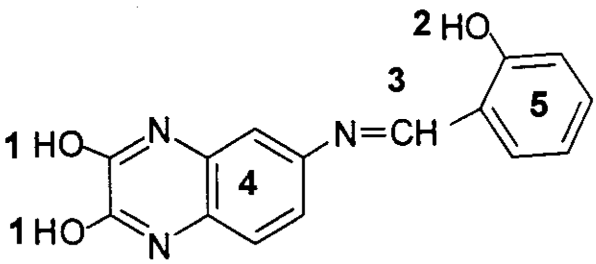

IIa

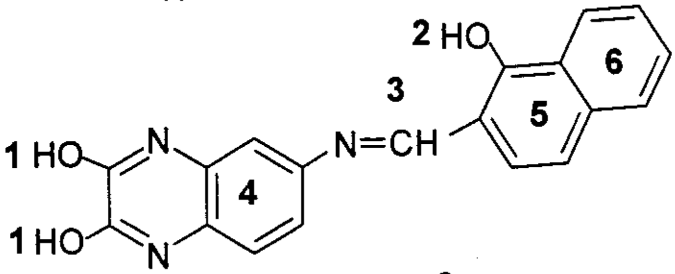

II_b

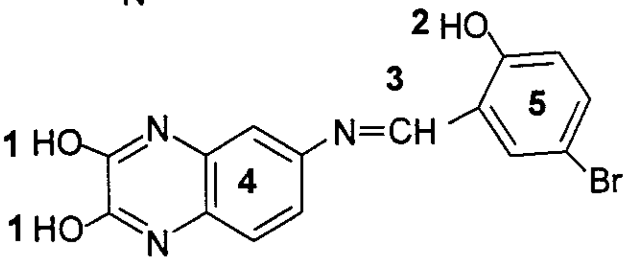

IIc

3.6.1. ¹H-NMR spectra of azo dyes compounds (I_{a-b})

The different types of signals for the hydrogens which are expected for the azo dyes compounds are shown in Fig. (18) and the chemical shift of different types of protons are recorded in Table (13). Also, the hydrogen magnetic resonance spectra of I_a and I_b on deuteration with D_2O are shown in Fig. (18). All signals observed take the integration value which give evidence and helps to assign the signals. The signals lying at very downfield side 13.2 and 10.0 ppm respectively for I_a and I_b are removed after deuteration which give evidence that they are due to the hydrogens of OH groups which are attached either to quinoxaline system or naphthalene system. On going from ligand I_a or I_b a new multiple signals at ranges 6.60-8.23 and 6.50-7.80 ppm, respectively which is due to the protons of the phenyl group didn't disappear after deuteration.

3.6.2. ¹H-NMR spectra of Schiff base compounds (II_{a-c})

The ¹H-NMR spectra of II_{a-c} as well as its deuteration by D_2O are shown in Figs. (18, 19) and chemical shift of the different signals are recorded in Table (13).

Also, it is clear from the ¹H-NMR spectra of II_a, II_b and II_c that the signals lying at very downfield side 10.24, 10.43 and 11.21 ppm respectively, which are removed on deuteration give evidence that they are due to the hydrogens of OH group which attached to the quinoxaline system, while the signals at 8.9, 9.6 and 12.04 ppm are due to the OH group which is attached to the phenyl ring in case of II_a, and II_c and to the naphthalene system in case of II_b.

Also, in ligand II_c the signal of OH group at 12.04 ppm was downfield side compared with the other two Schiff base ligands which is due to the presence of the bromide atom in para position which can withdraw the electron cloud from the aromatic ring this affect the OH group.

The signals observed at 6.7, 6.56 and 6.64 ppm were due to the azomethene group of ligands II_a, II_b and II_c respectively.

Table (13): ***Assignment and chemical shift (ppm) of different types of protons of ligands under investigation.***

Compound	Chemical shift (δ) (ppm) of protons					
	$H(1)_{OH}$	$H(2)_{OH}$	$H(3)_{=CH}$	H (4)	H (5)	H (6)
I_a	10.12, 10.23	13.20	-	6.60, 6.69, 6.64	8.06, 8.19, 8.23	7.70, 7.43, 7.63
I_b	9.80	-	-	7.80	7.40	6.50
II_a	10.24	8.97	6.70	8.02, 7.90, 7.72	7.20, 7.32, 7.53	-
II_b	10.43	9.62	6.56	7.61, 7.51, 7.42	7.92, 7.83, 7.73	7.23, 6.94, 7.11
II_c	11.21	12.04	6.64	7.19, 7.23, 6.92	7.80, 7.62, 7.89	-

Proton magnetic resonance of reagents under consideration

II_c with D_2O

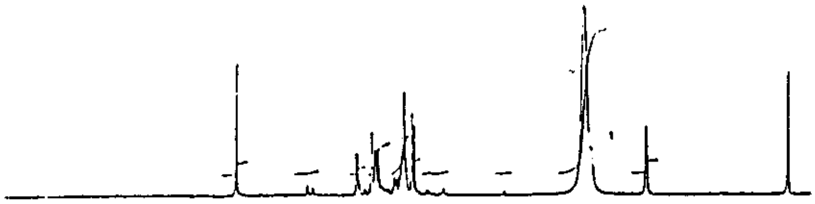

II_c

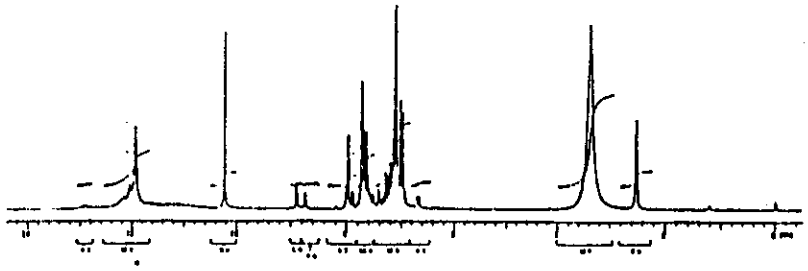

I_b

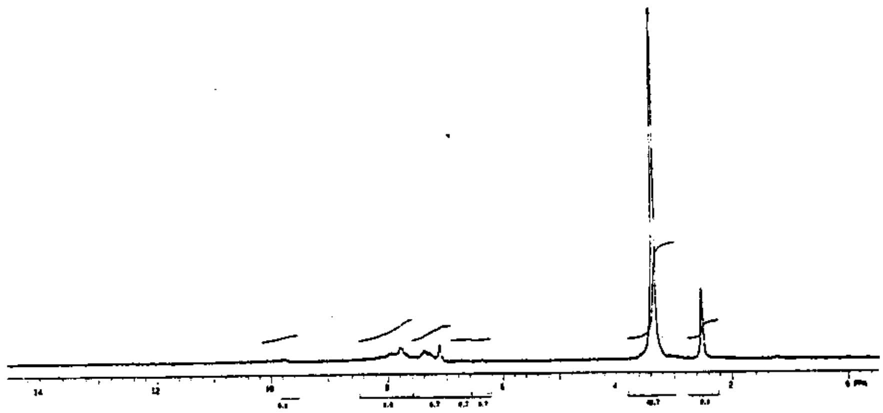

I_a

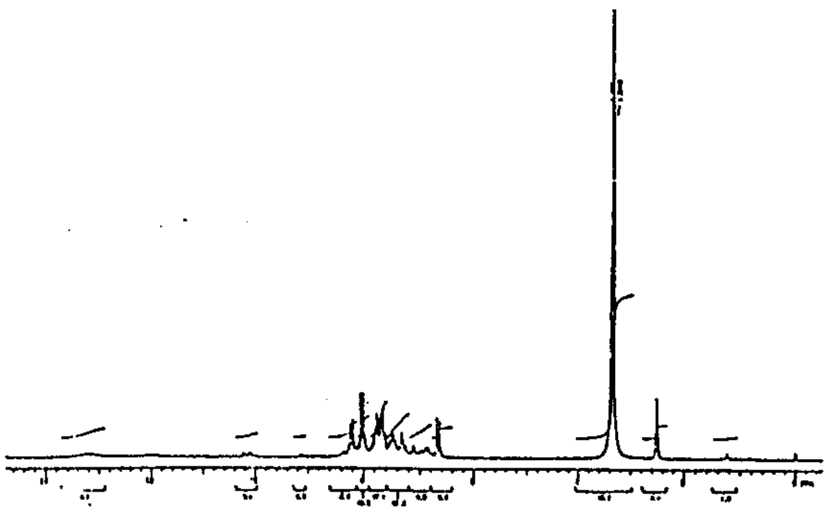

Fig. (18)

Proton magnetic resonance of reagents under consideration

II_a with D_2O

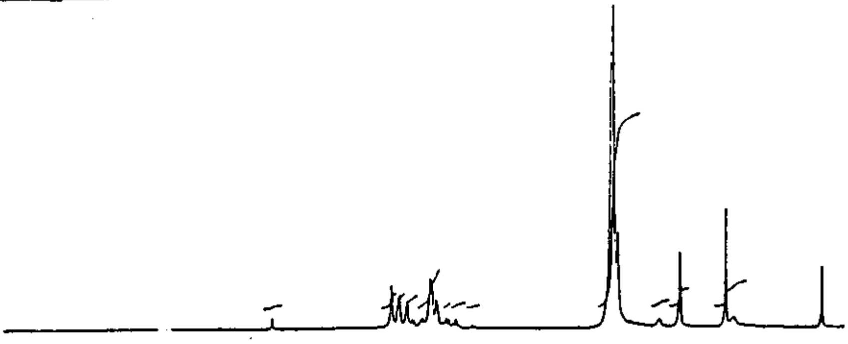

II_a

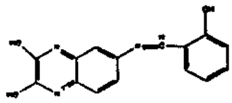

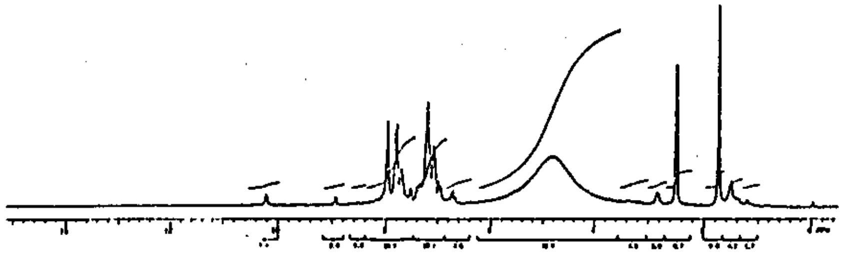

II_b with D_2O

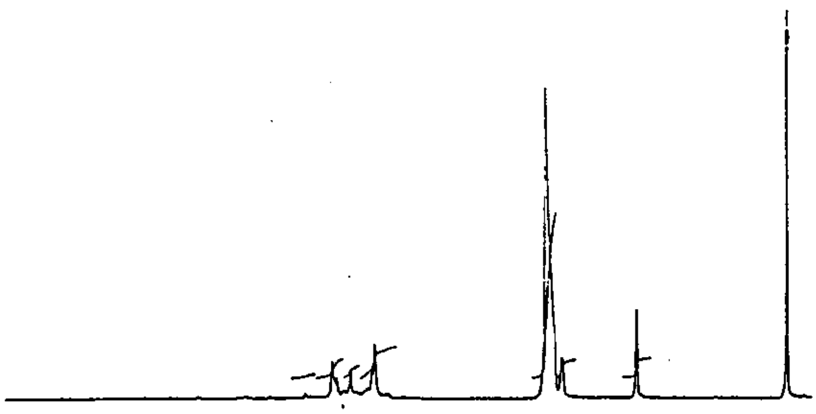

II_b

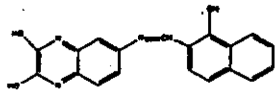

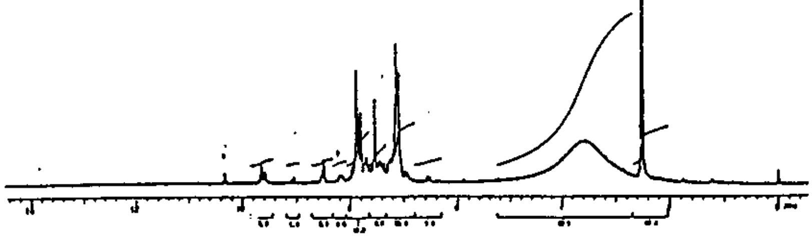

Fig. (19)

3.7. Cyclic voltammetry of free ligands

The electrochemical behavior of ligands, I_a, I_c, II_a and II_b was studied by cyclic voltammerty in 30 % ethanol using B-R buffer solutions in the pH range 2.3 - 11.3.

3.7.1. Cyclic voltammetric behavior of ligands I_a and I_c

Typical cyclic voltammograms obtained for 1 x 10^{-4} M solutions of ligands I_a and I_c are shown in Figs. (20-22) respectively. One well-defined reduction peak was obtained at about -630 mV for I_a and at about -50 mV for I_c along the entire pH range. In the reverse direction, one anodic peak was observed at about +400 mV for I_c The height of the oxidation peak is about half the height of the reduction wave in case of I_a and about the same height in case of I_c.

The dependence of cathodic peak currents (I_{pc}) and anodic peak currents (I_{pa}) on the pH are shown in Figs. (21, 23).

The effect of scan rate (ν) on the cyclic voltammetric parameters was investigated for I_a and I_c at pH 6.70 and 6.05, respectively. The reduction peak current I_{pc} is a linear function of $\nu^{1/2}$ for the two ligands under consideration, indicating that the reduction process is controlled mainly by diffusion. The shift of E_p to more negative potentials is an evidence for the irreversible nature of the electrode reaction.

The ratio of the anodic-to-cathodic peak heights (I_{pa}/I_{pc}) for the two ligands remains uncharged with the change of scan rate (ν). The reduction potentials for the reduction peak shifts to more negative values, while the oxidation potential for the oxidation peak shifts to more positive values on increasing ν, for the both ligands under investigation.

The influence of pH on the peak potential (E_P) and peak current (I_P) was investigated at ν = 200, 500 mVs^{-1} for I_a and I_c, respectively. The potential of the cathodic peak (I_{pc}) shifts towards more negative values as pH increases for the two ligands examined, resulting in a linear plot of mV per pH unit with slope equal to αn where α is the charge transfer rate constant and n the number of electrons involved in electron transfer processes. This indicates that hydrogen ions are involved in the electrode reaction [97].

From polarographic and voltammetric measurements of several azo compounds, it is known that the reduction of aromatic azo compounds containing electron donating substituents, such as hydroxyl groups, involve a cleavage of the azo bridge to yield the corresponding amines in acidic solutions. On increasing the pH, the reduction of the azo compound stops at the hydrazo step. The cleavage of the azo bridge should be a four electron process, while a saturation to hydrazo involves only two electrons[98, 99].

According to the data obtained from cyclic voltammetry, the reduction mechanism can be suggested as:

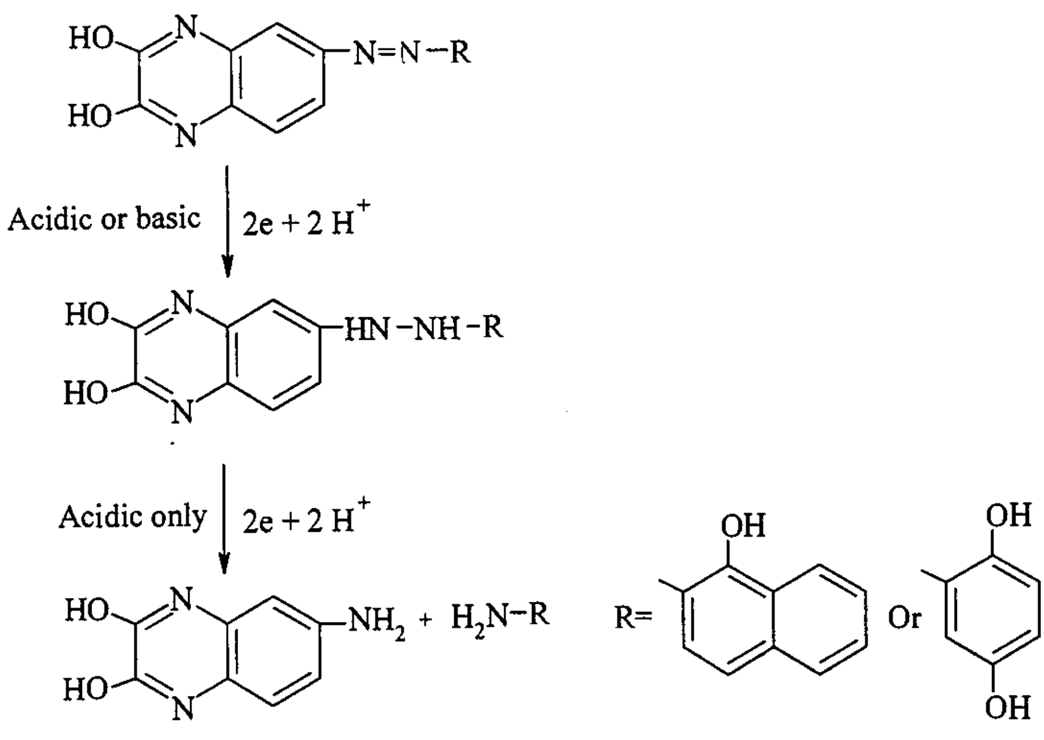

3.7.2. Cyclic voltammetric behavior of ligands II_a and II_b.

The cyclic voltammogrames of 1 x 10^{-4} M ligands II_a and II_b were recorded in B-R buffer over the pH range 2.5-11.3, Figs. (24, 26). For the two compounds, cyclic voltmmograms at 200 mVs^{-1} consist of a single cathodic wave at potentials at about -800 and -750 mV for II_a and II_b, respectively. No anodic wave occurs in the reverse scan direction. This behavior was observed for a wide range of scan rates from 50 to 1000 mVs^{-1}. Hence, such a reduction process should correspond to a totally irreversible electron transfer. The dependence of the cathodic peak currents on pH of the two ligands are shown in Figs. (25, 27).

The plot I_{pc} vs. $v^{1/2}$ showed a linear variation due to a diffusion-controlled mechanism. On the other hand, E_{pc} was independent of log v between 50-1000 mVs^{-1}.

The cathodic peak is due to the reduction of the imine bond, C=N of the ligands II_a and II_b. The reduction mechanism for the two ligands can be suggested as:

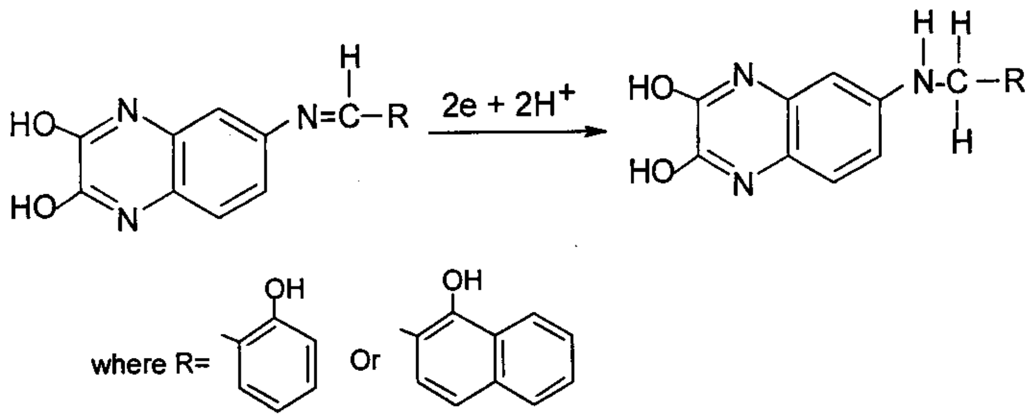

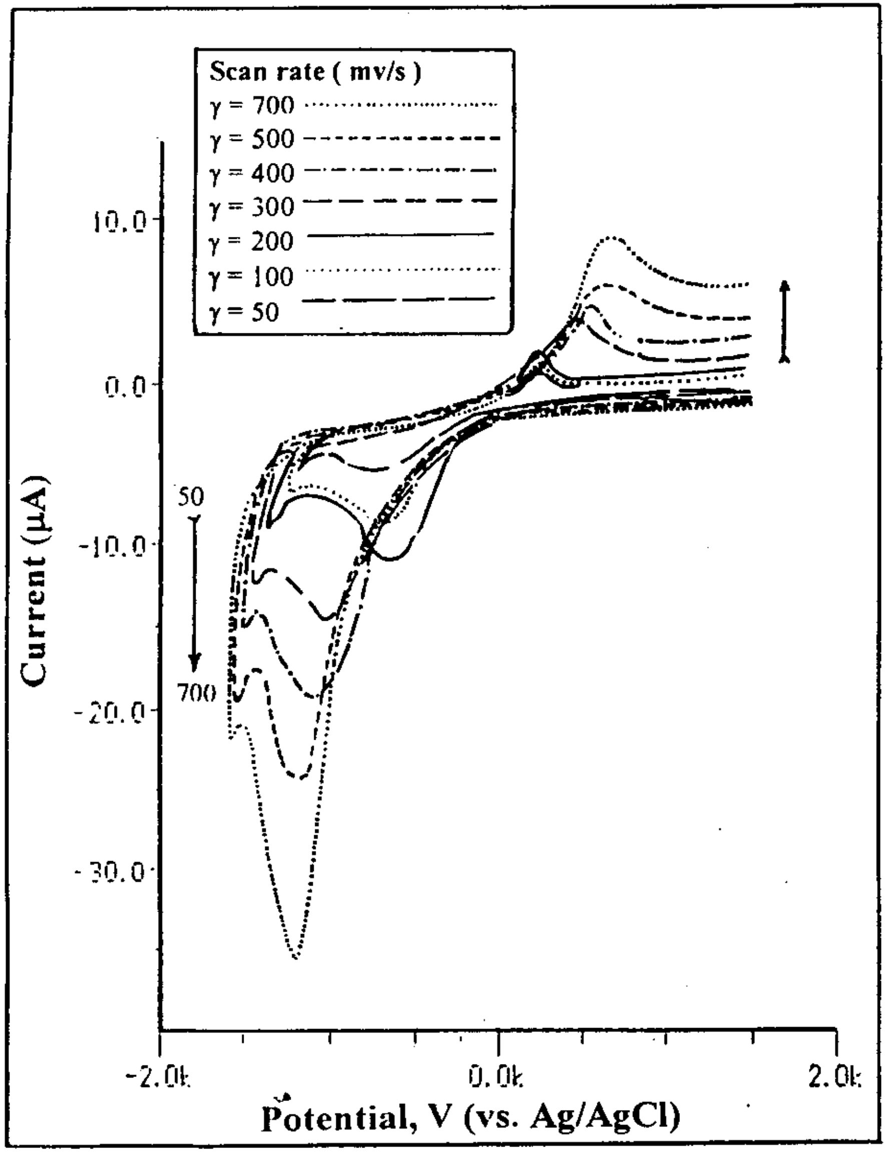

The effect of scan rate on cyclic voltammogram recorded on ligand (I_a) in 30% ethanol using a glassy carbon electrode
pH: 6.7

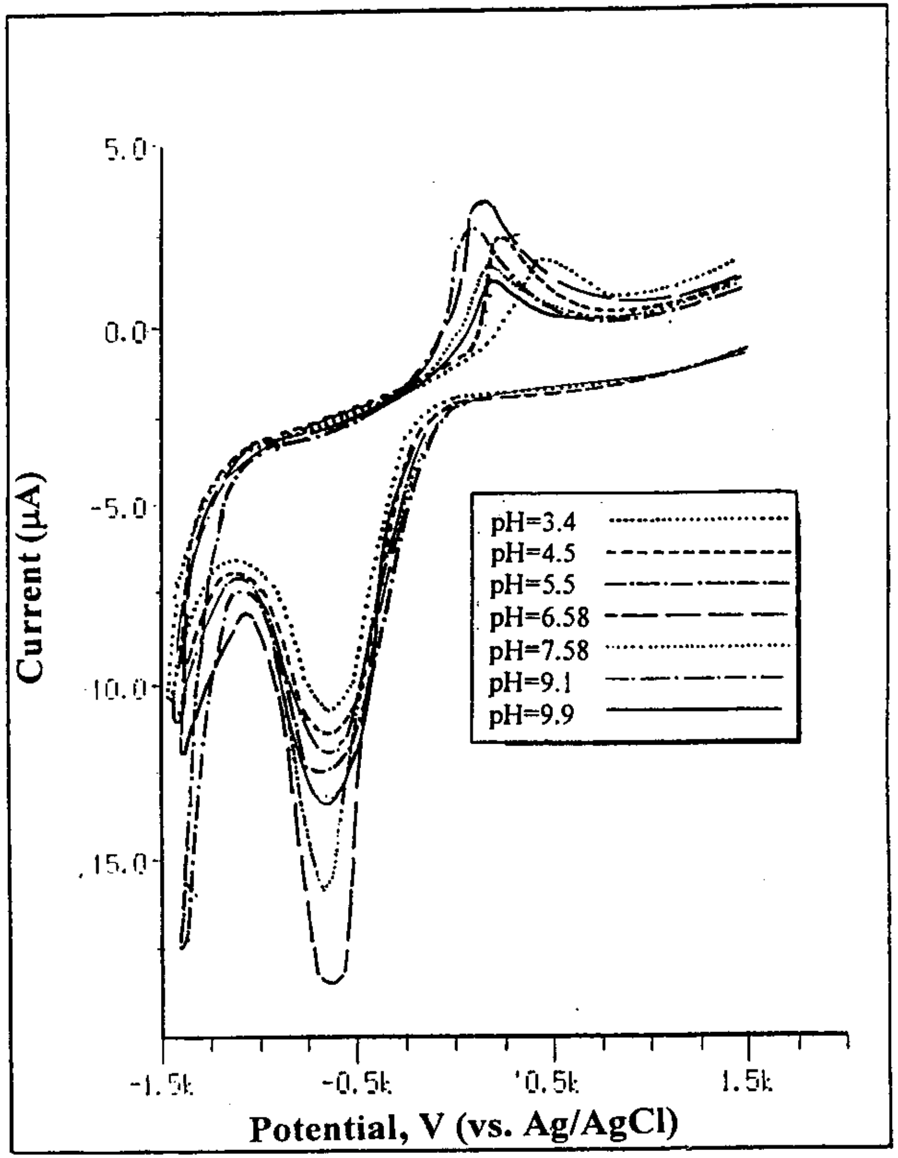

The effect of pH on cyclic voltammogram recorded on ligand (I_a) in 30% ethanol using a glassy carbon electrode
Scan rate: 200 mv/s

Fig. (20)

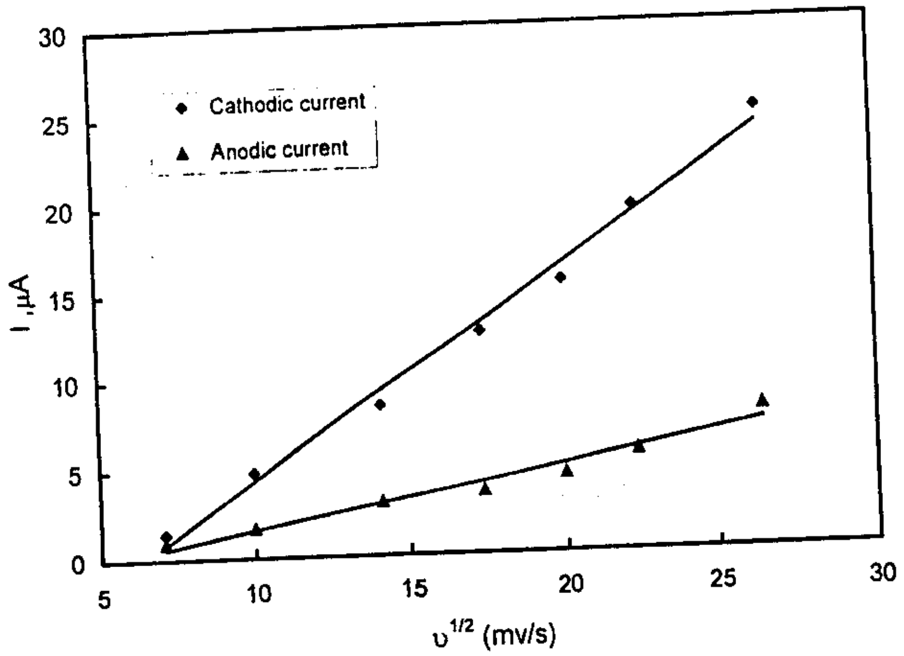

Cathodic current (i_{pc}) and anodic current (i_{pa}) vs. square root of sweep rate ($\upsilon^{1/2}$) for ligand I_a

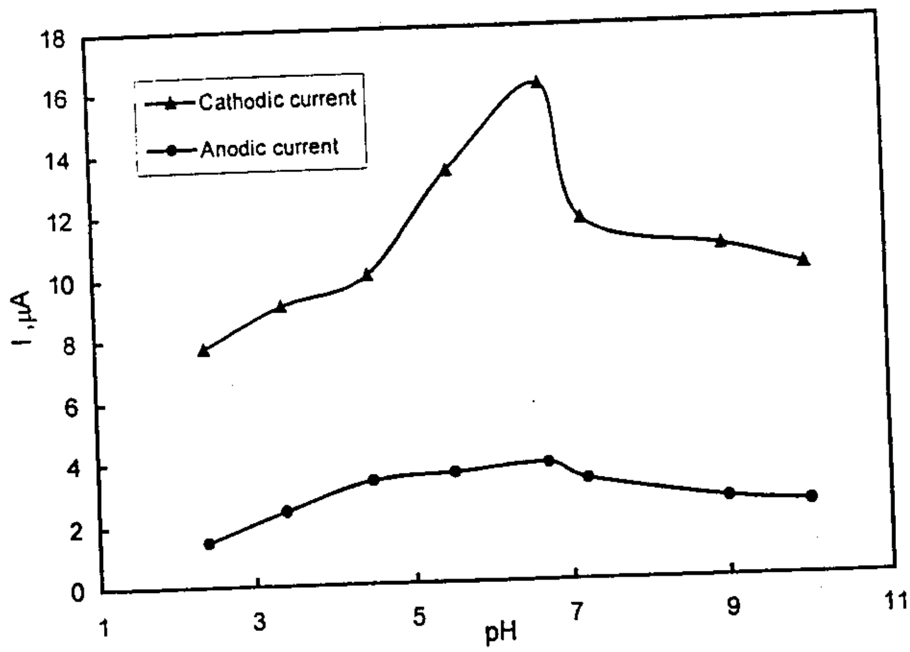

Relation between cathodic and anodic currents and pH for ligand I_a

Fig. (21)

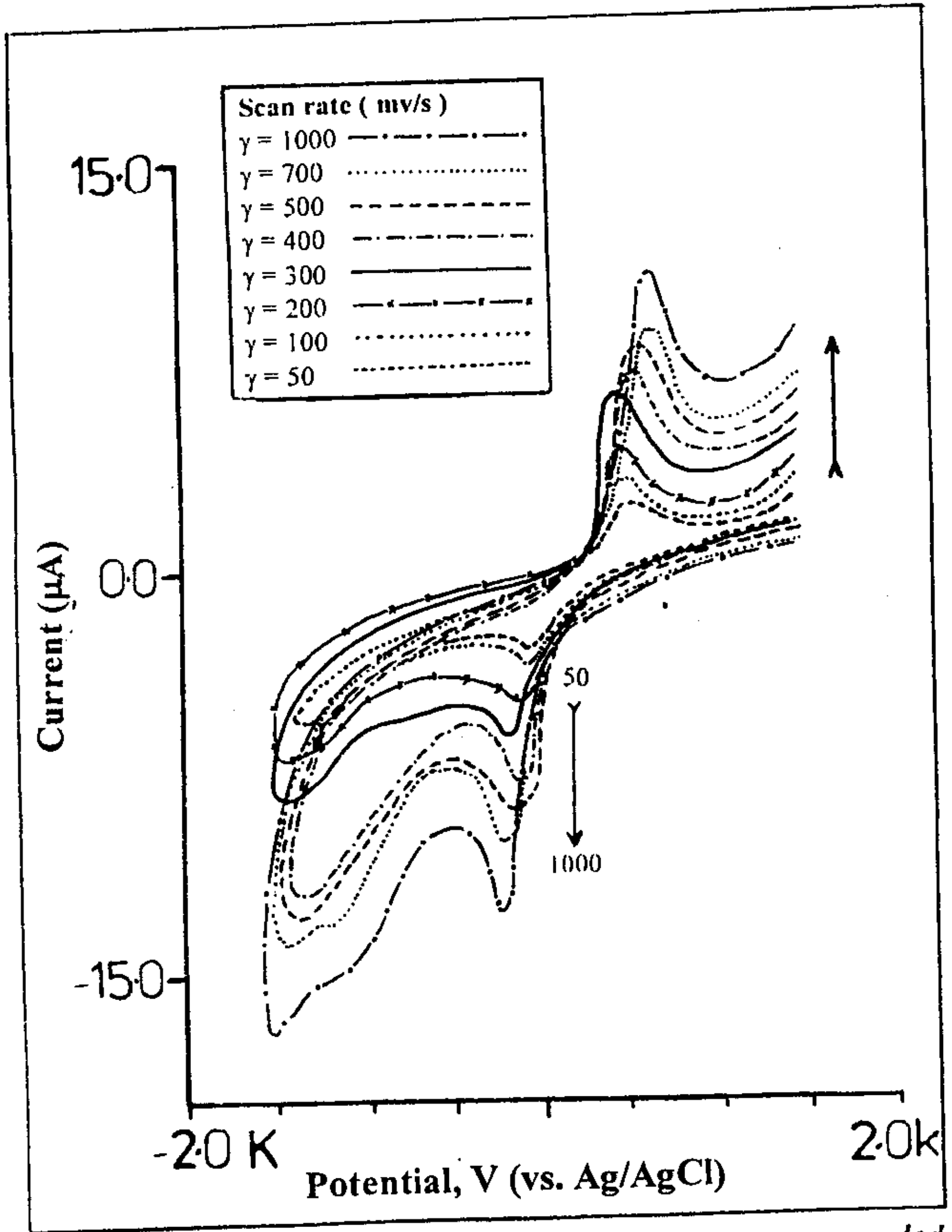

The effect of scan rate on cyclic voltammogram recorded on ligand (I_c) in 30% ethanol using a glassy carbon electrode
pH: 6.05

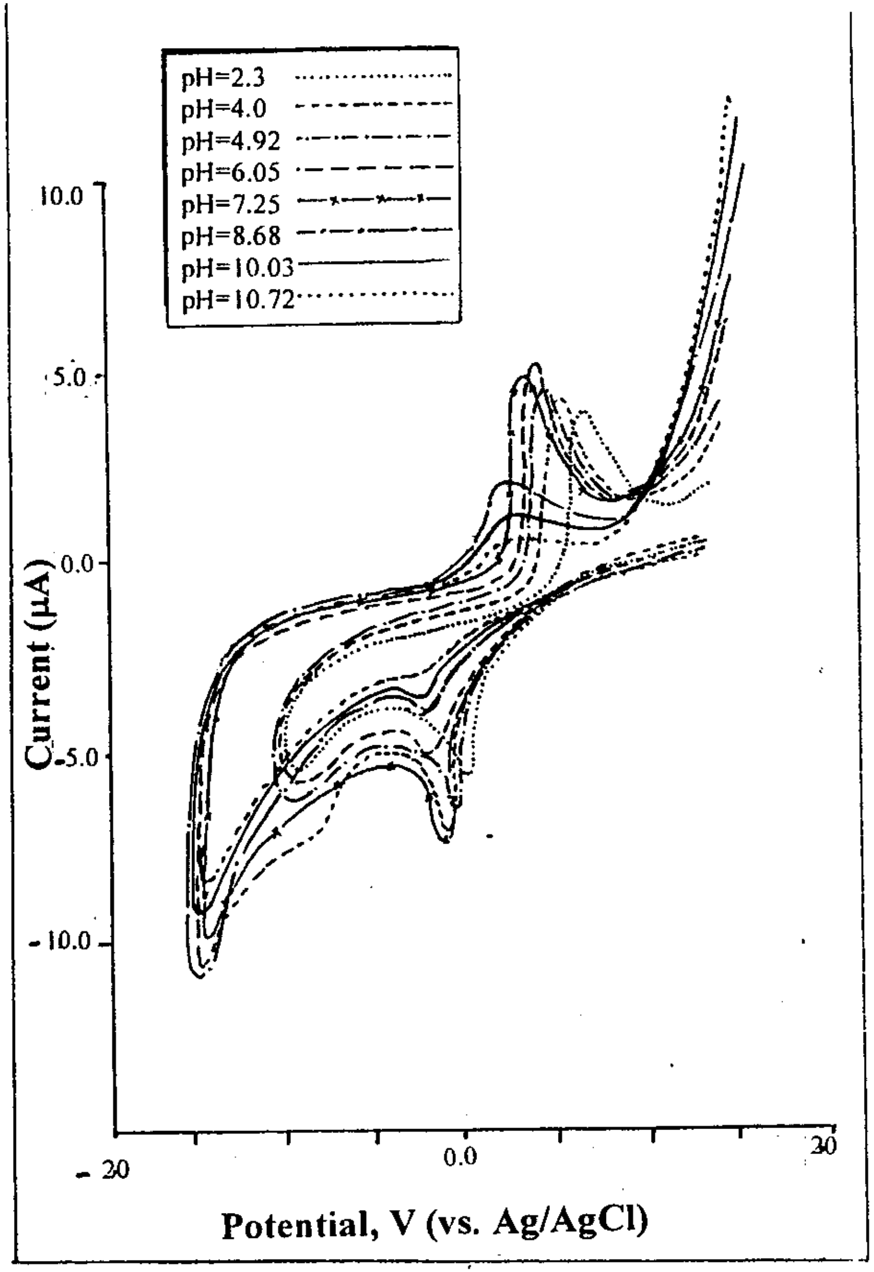

The effect of pH on cyclic voltammogram recorded on ligand (I_c) in 30% ethanol using a glassy carbon electrode
Scan rate: 500 mv/s

Fig. (22)

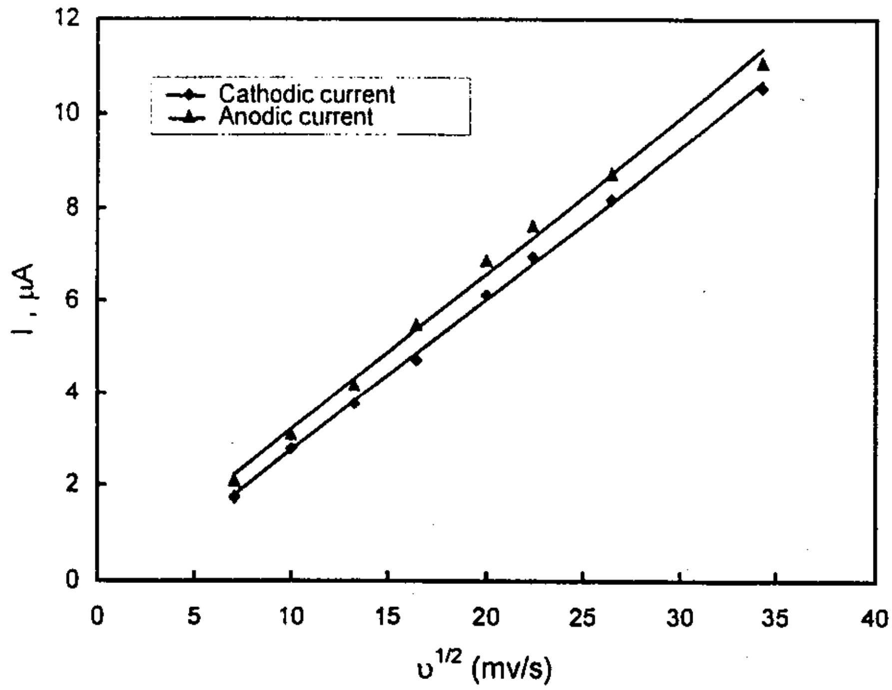

Cathodic current (i_{pc}) and anodic current (i_{pa}) vs. square root of sweep rate ($\upsilon^{1/2}$) for ligand I_c

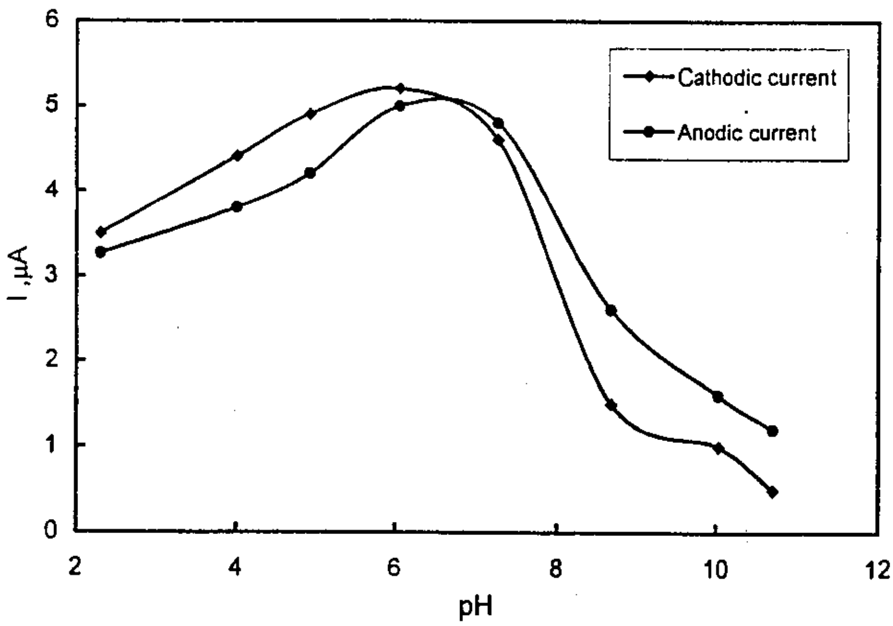

Relation between cathodic and anodic currents and pH for ligand I_c

Fig. (23)

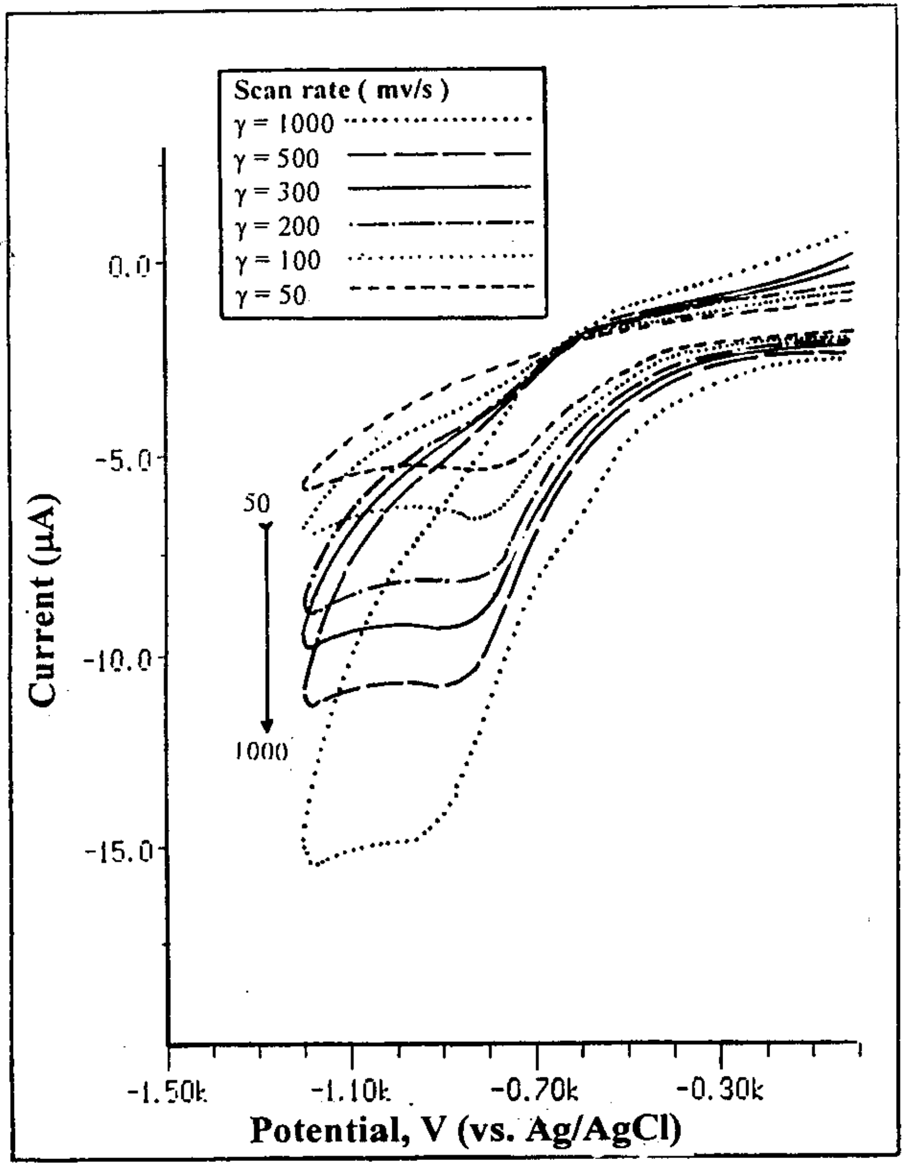

The effect of scan rate on cyclic voltammogram recorded on ligand (II_a) in 30% ethanol using a glassy carbon electrode at room pH: 7.6

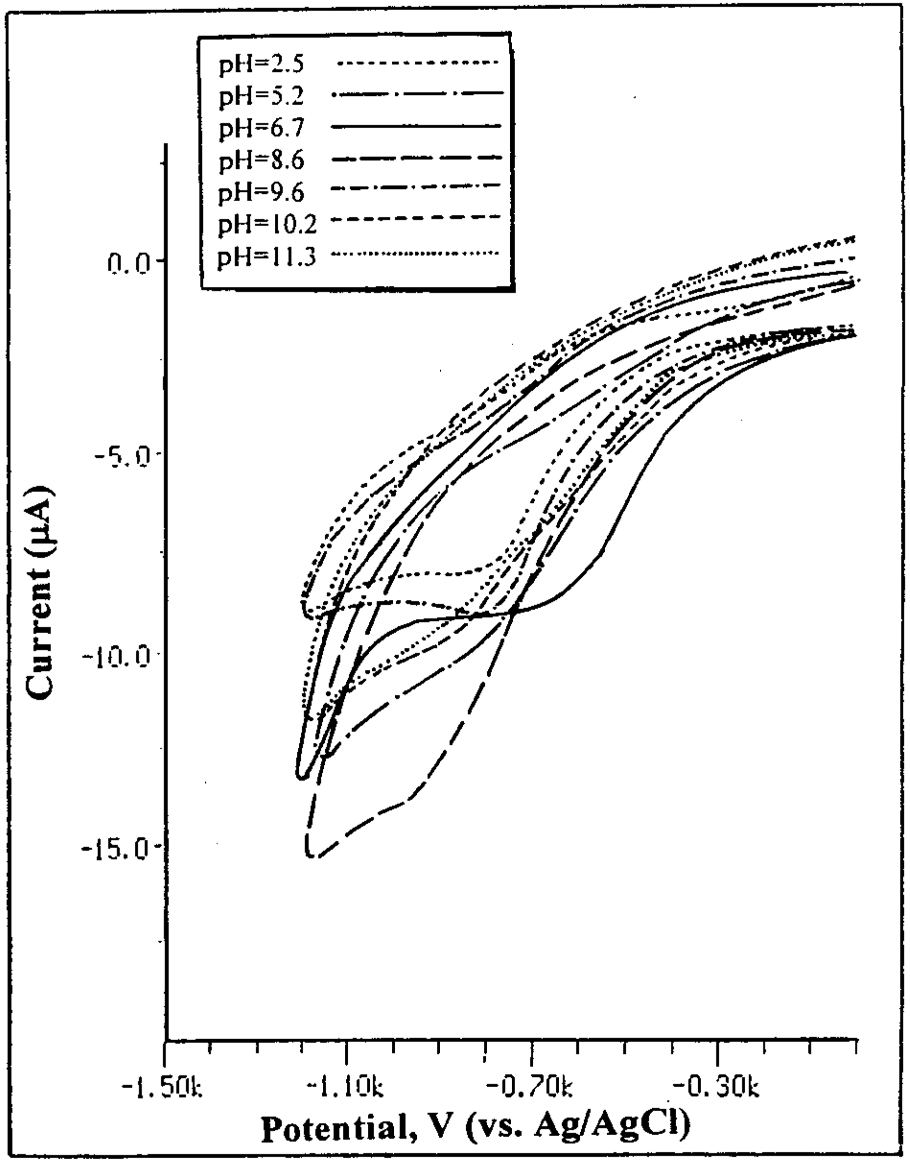

The effect of pH on cyclic voltammogram recorded on ligand (II_a) in 30% ethanol using a glassy carbon electrode
Scan rate: 200 mv/s

Fig. (24)

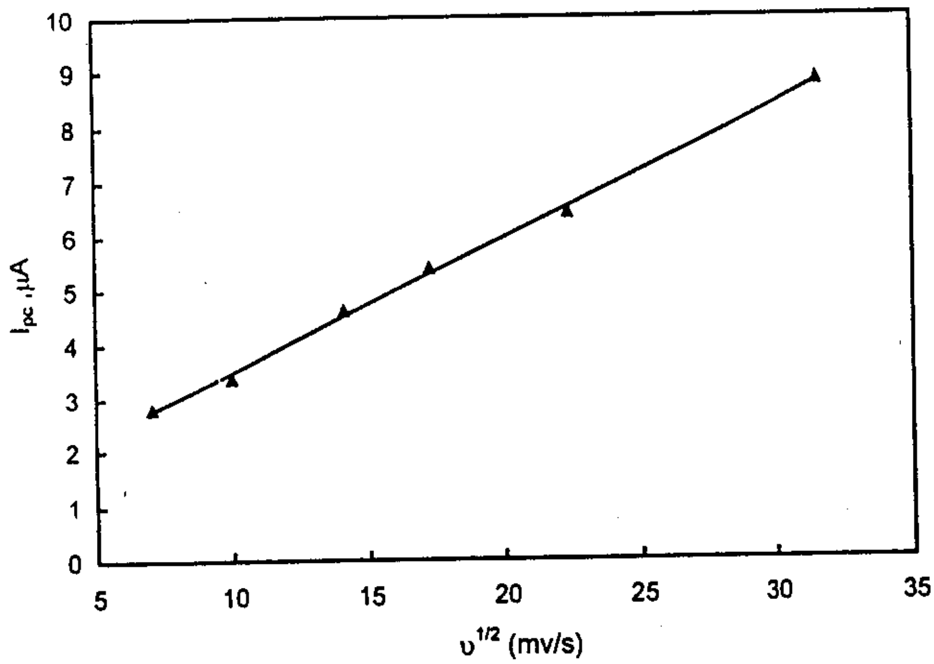

Cathodic current (i_{pc}) vs. square root of sweep rate ($\upsilon^{1/2}$) for ligand II_a

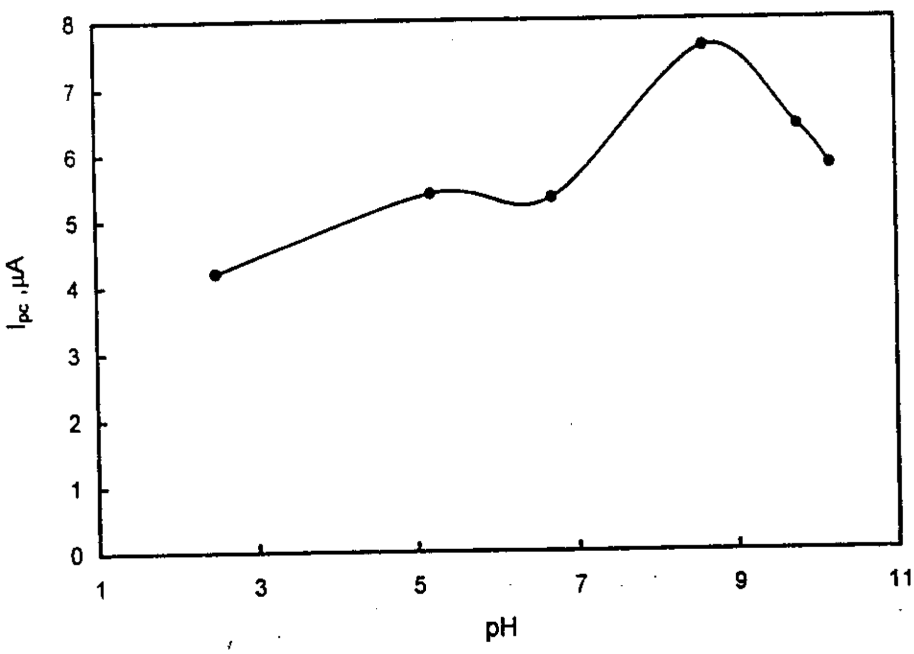

Relation between cathodic current and pH for ligand II_a

Fig. (25)

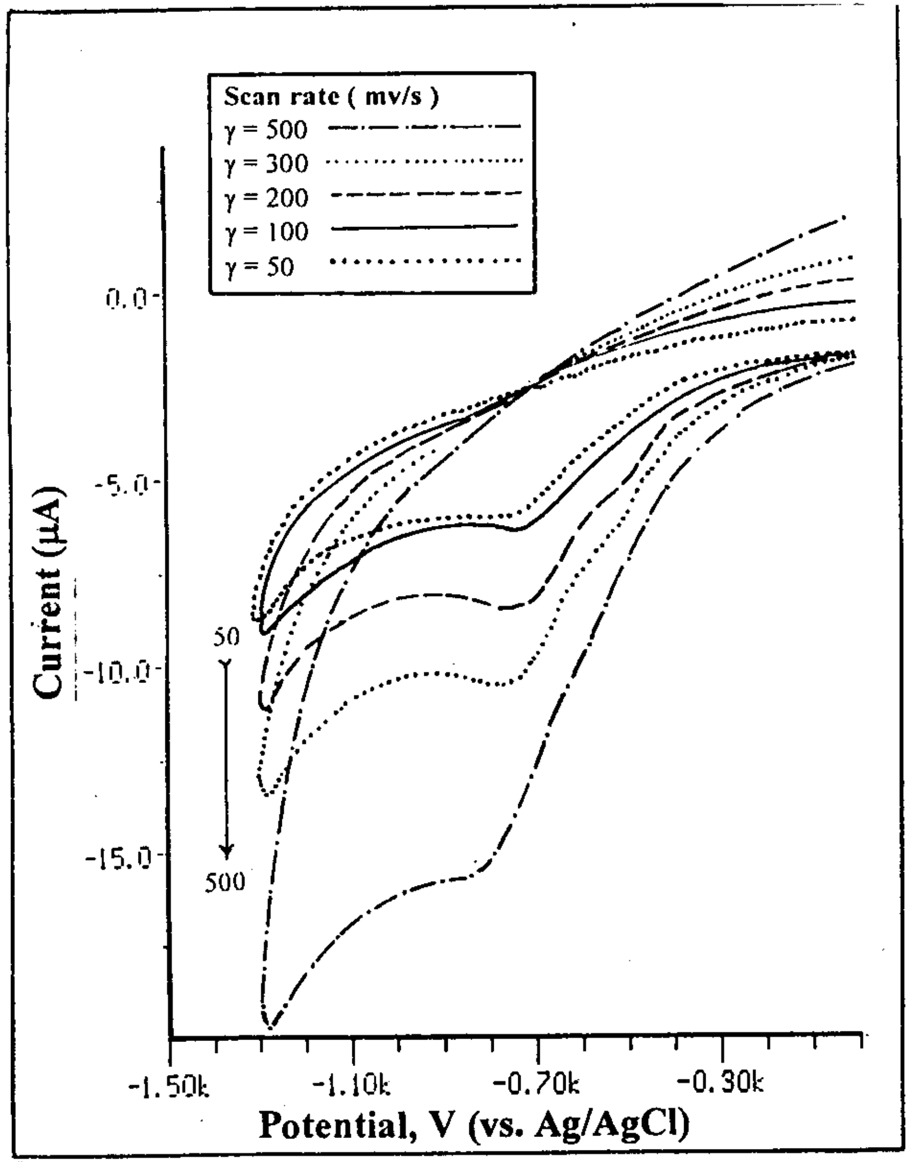

The effect of scan rate on cyclic voltammogram recorded on ligand (II_b) in 30% ethanol using a glassy carbon electrode
pH: 7.2

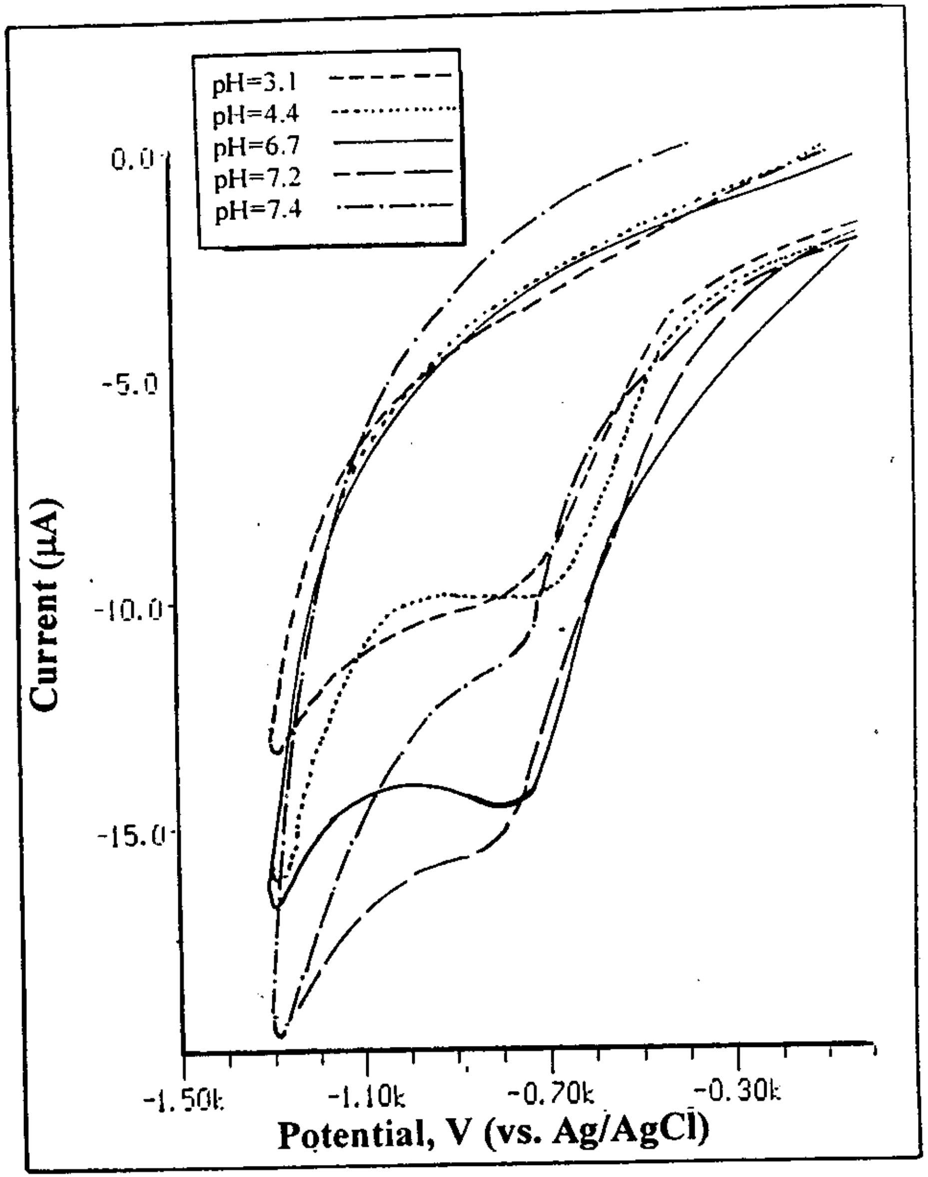

The effect of pH on cyclic voltammogram recorded on ligand (II_b) in 30% ethanol using a glassy carbon electrode
Scan rate: 500 mv/s

Fig. (26)

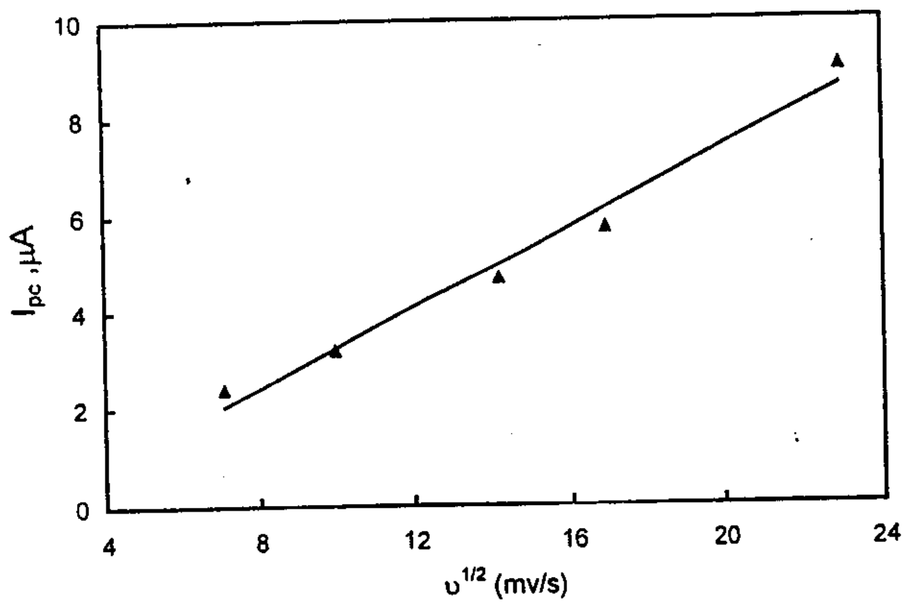

Cathodic current (i_{pc}) vs. square root of sweep rate ($\upsilon^{1/2}$) for ligand II_b

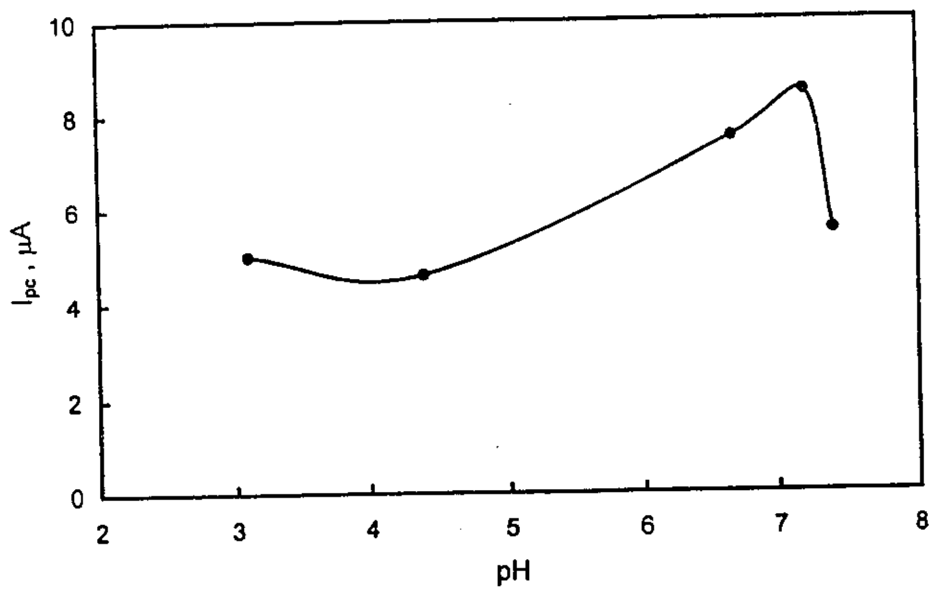

Relation between cathodic current and pH for ligand II_b

Fig. (27)